NEUROSCIENCE

RESEARCH ARTICLE

Melek Umay Tuz- Sasik et al. / Neuroscience 436 (2020) 46–73

Expression Levels of SMAD Specific E3 Ubiquitin Protein Ligase 2 (Smurf2) and its Interacting Partners Show Region-specific Alterations During Brain Aging

Melek Umay Tuz-Sasik, [a,b,c] **Elif Tugce Karoglu-Eravsar,** [a,b,c,d] **Meric Kinali,** [e] **Ayca Arslan-Ergul** [f] **and Michelle M. Adams** [a,b,c,g*]

[a] *Interdisciplinary Program in Neuroscience, Aysel Sabuncu Brain Research Center, Bilkent University, Ankara, Turkey*

[b] *National Nanotechnology Research Center (UNAM), Bilkent University, Ankara, Turkey*

[c] *Department of Molecular Biology and Genetics, Zebrafish Facility, Bilkent University, Ankara, Turkey*

[d] *Department of Psychology, Selcuk University, Konya, Turkey*

[e] *Graduate School of Informatics, Department of Health Informatics, Middle East Technical University, Ankara, Turkey*

[f] *Stem Cell Research and Application Center, Hacettepe University, Ankara, Turkey*

[g] *Department of Psychology, Bilkent University, Ankara, Turkey*

Abstract—Aging occurs due to a combination of several factors, such as telomere attrition, cellular senescence, and stem cell exhaustion. The telomere attrition-dependent cellular senescence is regulated by increased levels of *SMAD specific E3 ubiquitin protein ligase 2* (*smurf2*). With age s*murf2* expression increases and Smurf2 protein interacts with several regulatory proteins including, Smad7, Ep300, Yy1, Sirt1, Mdm2, and Tp53, likely affecting its function related to cellular aging. The current study aimed at analyzing *smurf2* expression in the aged brain because of its potential regulatory roles in the cellular aging process. Zebrafish were used because like humans they age gradually and their genome has 70% similarity. In the current study, we demonstrated that *smurf2* gene and protein expression levels altered in a region-specific manner during the aging process. Also, in both young and old brains, Smurf2 protein was enriched in the cytosol. These results imply that during aging Smurf2 is regulated by several mechanisms including post-translational modifications (PTMs) and complex formation. Also, the expression levels of its interacting partners defined by the STRING database, *tp53*, *mdm2*, *ep300a*, *yy1a*, *smad7*, and *sirt1*, were analyzed. Multivariate analysis indicated that *smurf2*, *ep300a*, and *sirt1*, whose proteins regulate ubiquitination, acetylation, and deacetylation of target proteins including Smad7 and Tp53, showed age- and brain region-dependent patterns. Our data suggest a likely balance between Smurf2- and Mdm2-mediated ubiquitination, and Ep300a-mediated acetylation/Sirt1-mediated deacetylation, which most possibly affects the functionality of other interacting partners in regulating cellular and synaptic aging and ultimately cognitive dysfunction.

Key words: ***Smurf2*, *Mdm2*, *Ep300a*, *Sirt1*, aging, zebrafish.**

INTRODUCTION

Aging is a natural and multi-factorial process that is accompanied by numerous alterations in the organism. At a systems level, normal aging is associated with changes in cognitive function, which include slowing down of information processing, moderate declines in memory, and increased failure in executive functions (Raz, 2002). Normal aging leads to a measurable but tolerable loss of cognitive ability that may or may not affect the person's quality of life or ability to function and identifying the cellular mechanisms that underlie these cognitive changes will be vital to preserving an older person's independence.

At a macroscopic level, it has been suggested that significant cellular and synaptic loss underlie these altered cognitive functions. However multiple studies indicate that there is no significant cellular (Rapp and Gallagher, 1996; Rapp et al., 2002) and synaptic loss (Calhoun et al., 1998; Poe et al., 2001; Shi et al., 2007;

*Correspondence to: M. M. Adams, Interdisciplinary Graduate Program in Neuroscience, Aysel Sabuncu Brain Research Center, Bilkent University, 06800 Bilkent, Ankara, Turkey.
E-mail address: michelle@bilkent.edu.tr (M. M. Adams).

Abbreviations: HSCs, hematopoietic stem cells; LTP, long-term potentiation; MDM2, mouse double minute 2; NAD, nicotinamide adenine dinucleotide; NSCs, neural stem cells; PCA, Principal Component Analysis; PTMs, post-translational modifications; TGF-β, transforming growth factor-β; tp53, tumor protein p53.

https://doi.org/10.1016/j.neuroscience.2020.04.003
0306-4522/

Newton et al., 2008) in the aged brain. Thus, it is likely subtle cellular and synaptic alterations are contributing to this brain aging process (Ganeshina et al., 2004; Adams et al., 2008; VanGuilder et al., 2010, 2011). Therefore, analyzing subtle molecular and cellular alterations in the aged brain, rather than focusing on significant structural changes, will provide powerful insights for understanding the neurobiological underpinnings of the aging process.

Some of the widely-accepted hallmarks of aging demonstrate shared characteristic features of age-related cellular changes in the brain, and may contribute to the subtle functional alterations in neuronal cellular and synaptic integrity. Genomic instability and telomere attrition are defined as the primary hallmarks of aging because they lead to cellular damage and dysfunction, and ultimately cellular senescence (López-Otín et al., 2013). Due to endogenous risk factors such as DNA replication errors and reactive oxygen species, as well as exogenous biological, chemical and physical risk factors, the cellular mechanisms maintaining DNA integrity and stability are subject to dysfunction during the aging process (Hoeijmakers, 2009). Throughout the life of an organism, genetic damage accumulates in the cells, and thus, cellular aging results from a buildup of many years of DNA damage. A complex DNA repair system network maintains genomic stability in normal cells (Lord and Ashworth, 2012). In addition to DNA repair processes, specific mechanisms for preserving the integrity and length of telomeres have evolved (Blackburn et al., 2006). Although telomere attrition increases with advancing age in mammals because of the end replication problem in each DNA replication cycle (Levy et al., 1992), it is long discussed whether telomere attrition is a cause of aging or consequence of aging (Hornsby, 2006; Carneiro et al., 2016). Although telomerase, a specialized DNA polymerase, may overcome this problem, most somatic cells in mammals lose the ability of telomerase expression by maturation (Wright et al., 1996; Cong et al., 2002). In the absence of telomerase, the shortening of telomeres increases throughout life. Evidence from previous literature indicates that telomere attrition is a feature of replication-competent cells such as small intestine and ovaries; however, recent findings demonstrate that post-mitotic neurons may also display senescence-like characteristics due to telomere erosion (Ain et al., 2018). The response to both genomic instability and telomere attrition in the cell could be in some cases to undergo cellular senescence, which is considered another hallmark of aging (López-Otín et al., 2013). Senescent cells accumulate in aged tissues because of either an increase in their generation or a decrease in their clearance (López-Otín et al., 2013). Additionally, with an increase in senescent cells, the regenerative potential of tissues declines during aging. For example, the generation of hematopoietic stem cells (HSCs) declines with age and this leads to alterations in the production of immune cells, which is known as immunosenescence (Shaw et al., 2010; Fulop et al., 2018). Interestingly, recent findings imply a protective role of senescence in tissue repair and regeneration. It has been shown that senescent cells in a wounded tissue increase myofibroblast differentiation, and fastens wound healing (Demaria et al., 2014). Similarly, it was found that senescence may act to prevent injury-associated tissue fibrosis by restraining proliferation (Krizhanovsky et al., 2008).

In conjunction with these changes, some common factors have the ability to regulate all the hallmarks of aging mentioned above. One such component is the SMAD specific E3 ubiquitin protein ligase 2 (Smurf2), which regulates ubiquitin-mediated proteasomal degradation. Evidence shows that Smurf2 protein has roles in both the induction of telomere-dependent cellular senescence (Zhang and Cohen, 2004) and stem cell exhaustion (Ramkumar et al., 2014). Moreover, gene expression levels of *smurf2* are significantly increased in the aged brain (Arslan-Ergul and Adams, 2014). This suggests a potential role for this protein in mediating some of the functional changes associated with cellular aging.

Smurf2 is a conserved 'homologous to E6-AP COOH terminus' (HECT)-domain E3 ubiquitin ligase protein belonging to the Nedd4 subgroup (Chen and Matesic, 2007). It was first identified as a negative regulator of transforming growth factor-β (TGF-β) signaling by targeting receptor-regulated Smads and the TGF-β type I receptor (Zhang et al., 2001). It implemented this through interactions with phosphorylated Smads, which leads to their ubiquitination and subsequent degradation (David et al., 2013). Nuclear export of Smurf2 requires an association with Smad7 that leads to ubiquitin-mediated proteasomal degradation of TGF-β receptor complex (Kavsak et al., 2000; Yan et al., 2009). Thus, Smurf2 can be found in nuclear and cytosolic fractions depending on the cellular conditions (Borroni et al., 2018; Emanuelli et al., 2019). Further research demonstrated that Smurf2 has essential roles in other signaling pathways and cellular processes such as telomere attrition and induction of cellular senescence. For example, telomere attrition occurs in parallel with an increase in Smurf2 expression, both of which are sufficient for the development of a senescent phenotype, and ectopic expression of Smurf2 in early passage fibroblast cells leads to cellular senescence (Zhang and Cohen, 2004). Several studies have increased our understanding of the function of Smurf2 as being related to cellular senescence, it has been shown that it mechanistically links to p16 (Kong et al., 2011), which is considered as a marker of aging (Krishnamurthy et al., 2004). The gene expression levels of *p16* increase in cells undergoing senescence (Krishnamurthy et al., 2004) and this leads to a decrease in the self-renewal capacity of stem cells during aging (Ramkumar et al., 2014). Taken together, these data suggest that Smurf2 may promote an aging phenotype of cellular senescence through telomere attrition.

In promoting cellular senescence, not only is the p16 pathway recruited by Smurf2 but it also regulates and recruits the p53-p21 pathway (David et al., 2013). A well-studied transcription factor, tp53, responds to several cellular stressors by regulating target genes, which induce growth arrest, DNA repair, cellular senescence, and apoptosis (Li et al., 2002a). Smurf2 promotes tumor protein p53 (tp53) degradation by stabilizing the E3 ubiquitin

protein ligase 'mouse double minute 2' (MDM2) (Nie et al., 2010). Also, Yin Yang 1 (YY1), which is degraded by Smurf2, inhibits tp53 activity (Sui et al., 2004), and thus, the suppressive ability of YY1 on tp53 activity is relieved by Smurf2 (Jeong et al., 2014). Furthermore, as a stress response, tp53 is acetylated by E1A Binding Protein P300 (ep300), a transcriptional co-activator; however, MDM2 suppresses ep300-mediated tp53 acetylation (Ito et al., 2001). Smad7 is acetylated by ep300 to protect against Smurf2-mediated ubiquitination similarly to the tp53 regulation mentioned above (Grönroos et al., 2002; Simonsson et al., 2005). In contrast to ep300, Sirtuin 1 (SIRT1), a nicotinamide adenine dinucleotide (NAD)-dependent deacetylase, removes the acetyl groups from Smad7, which inhibits TGF-β signaling (Yan et al., 2009). It has been suggested that the sirtuin family, including SIRT1, regulates life span in concert with metabolism because of the NAD-dependent deacetylase function (Guarente, 2007). In addition to its role in metabolism, SIRT1 regulates senescence via deacetylation of target proteins (Yuan et al., 2016). All of these results suggest a role for Smurf2 and its downstream targets and interacting partners in controlling several hallmarks of aging such as telomere attrition, cellular senescence, genomic stability, and stem cell exhaustion. Despite the wealth of research investigating Smurf2 in relationship to these processes and cancer, the current study is one of the first to investigate alterations in *smurf2* expression in the aging brain.

The zebrafish (*Danio rerio*) model organism has begun to get attention as a gerontological model (Van houcke et al., 2015) because it has an integrated nervous system, and shows advanced behavioral properties such as memory and social behaviors (Saverino and Gerlai, 2008; Oliveira, 2013). Additionally, they age gradually like humans (Kishi et al., 2003), and their genome shows a 70% similarity with the human genome (Howe et al., 2013). Moreover, the zebrafish brain has regenerative properties, including neurogenesis that is not restricted to the telencephalon but is widespread throughout the entire brain (Kizil et al., 2012). Although these animals possess a high regenerative capacity (Johnson and Weston, 1995; Becker et al., 1997; Poss, 2002), neurogenesis decreases with age in zebrafish (Edelmann et al., 2013; Arslan-Ergul et al., 2016). This is in concert with increases in an important biomarker of aging, senescence-associated β-galactosidase (SA β-gal), which builds up linearly with advancing age in the zebrafish brain and other tissues (Kishi et al., 2008; Arslan-Ergul et al., 2016). As indicated in the review by Van houcke et al. (2015), these hallmarks of aging observed in mammals are well-represented in the zebrafish nervous system, and thus, they are a promising model organism to study brain aging and age-related changes.

In the light of all this evidence, we hypothesized that Smurf2 protein expression would increase in the aged brain in a manner similar to the mRNA levels, and this upregulation would influence Smurf2 interacting partners' gene expression levels. Western blot experiments were performed with two different anti-SMURF2 antibodies, which recognize different domains of the Smurf2 protein. Blots with the anti-SMURF2, 200–300 aa, antibody, which is recognizing the portion between the 200–300 amino acid residues of Smurf2 protein, showed that the expression levels did not change with age. However, the other antibody directed toward the C-terminal region yielded a band corresponding to a larger molecular weight protein and demonstrated a numerical but not statistically significant increase in the protein level of Smurf2 during aging. To further analyze the region-specific protein expression levels of Smurf2, proteins from microdissected brain regions including the telencephalon (Tel), optic tectum (TeO) and cerebellum/medulla/spinal cord (Ce) were analyzed with Western blotting of two antibodies directed against the Smurf2 protein. The analyses with both antibodies indicated a region-specific increase in Smurf2 protein expression during aging that was limited to the Tel region. In order to define the subcellular localization of Smurf2 with advancing age, fractionation experiments were performed on the whole brain and specific brain regions and it was indicated that the presence of enriched cytosolic levels of Smurf2 was observed in the whole brain and three specific brain regions. Moreover, since Smurf2 is known to regulate various functions in the cell through different targets, it was also important to define the downstream genes and interacting partners and measure their expression levels during brain aging. Using the STRING database (Szklarczyk et al., 2019), we generated a protein interaction map and measured the gene expression levels of *tp53*, *mdm2*, *sirt1*, *yy1a*, *ep300a*, and *smad7*, in addition to *smurf2*. While the whole brain expression analysis showed a numerical increase only in *smurf2* expression levels, the brain region-specific analysis indicated alterations in *mdm2*, *ep300a* and *sirt1* as well as *smurf2* expression levels varied during aging. Moreover, multivariate testing of gene expression levels using Principal Component Analysis (PCA) demonstrated that *smurf2*, *ep300a*, and *sirt1* influenced the variance in the same way in the whole brain, while each region had its own distinct pattern. This indicates that their regulatory roles are correlated with each other, i.e., all changed in the aging brain in region-dependent manner, and these changes in the interacting partners in the signaling pathway may influence cellular aging hallmarks such as senescence induced by telomere attrition or genomic instability.

EXPERIMENTAL PROCEDURES

Animals and cell lines

All fish were raised in standard conditions in the zebrafish facility in Bilkent University Molecular Biology and Genetics Department, Ankara, Turkey. Zebrafish were kept on a 14-hour light/10-hour dark cycle at a constant temperature of 27.5 °C. Adult fish were fed twice a day with dry food flakes and once a day with *Artemia*, which is live food and predatory source for the animals.

For the current study, both wild-type (AB strain) zebrafish embryos and larvae at 2, 3, and 4 days post fertilization (dpf), and brains from adult fish, which were

6–8 months old (young) and 29–35 months old (old), were examined. The age range of old group were determined according to previous research indicating that in zebrafish cognitive decline starts after 24 months and continue until 36 months (Yu et al., 2006). The adult brain tissue samples included both male and female animals. Both larvae and the adult fish were euthanized in ice water (American Veterinary Medical Association (AVMA), 2013; Varga and Matthews, 2012). After euthanization, embryos were pooled, snap-frozen in liquid nitrogen, and kept at −80 °C until protein extraction. Using the dissecting microscope, the head of the adult fish was removed from the body with a sharp blade after euthanization, and then the eyes and optic nerve were separated carefully from the head. After cleaning off the excessive tissues, the brain was removed from the skull in an entirely intact form. The brain weight was determined and recorded. Individual brain tissues were snap-frozen in liquid nitrogen and kept at −80 °C until further analysis for whole brain RNA isolation, while proteins were isolated from individual brain tissues immediately in lysis buffer. For region-specific RNA and protein isolation, three young and three old zebrafish brains were microdissected into three regions: telencephalon (Tel), the optic tectum (TeO) and the cerebellum/medulla/spinal cord (Ce). After Tel, TeO, and Ce were separated from each whole zebrafish brain sample, the 3 microdissected pieces from each of the three animals in the same age group were pooled together. Similar to whole brain RNA and protein isolation, pooled brain regions for RNA isolation were snap-frozen in liquid nitrogen and kept at −80 °C, while the proteins of the pooled brain regions were isolated immediately in the lysis buffer. For subcellular fractionation, dissected whole brains and three microdissected brain regions; Tel, TeO, and Ce, which were pooled, were lysed immediately. The animal protocol for this study was approved by the Bilkent University Local Animal Ethics Committee (HADYEK) with approval date Feb 21, 2018 and number 2018/5.

Different tissue cell lines were used for the validation of antibodies used in measuring the Smurf2 protein levels in the zebrafish brain tissues. The MDA-MB-231 cell line is a positive control for the anti-SMURF2 C-terminal (ab211746) antibody and the MCF7 cell line is a positive control for anti-SMURF2, 200–300 aa, (ab94483) antibody. These two breast cancer cell lines were kindly provided as cell pellets from Dr. Ali Gure's laboratory in Bilkent University. In order to show the expression of Smurf2 in brain cells, the A172, a human brain glioblastoma cell line, was used, which were in our laboratory.

Protein isolation for Smurf2 analysis

Protein isolation from individual and pooled brains was performed as described in Karoglu et al. (2017). Briefly, brain tissues were homogenized with a 25-gauge, 2-mL syringe in lysis RIPA buffer (50 mM Tris, pH 8.0, 150 mM NaCl, 1% NP40, 0.1% SDS and protease inhibitor [Roche, 5892970001]), for which 60 μL was used per 1 mg of tissue. Homogenates were incubated on ice for 30 min with gentle mixing. After centrifuging at 13,000 rpm for 20 min at 4 °C, supernatants were collected in a new tube. The only modification in the protocol was for protein isolation from the embryos. They were homogenized with a sonicator (UP 50H, Hielscher Ultrasonics GmbH, Teltow, Germany) in order to prevent the loss of sample that occurs with the use of a syringe during the protein extraction of pooled embryos. The protein extraction from the cell lines was performed in a similar manner for brain tissues as described above. The concentration of protein lysates was measured using the Bradford assay (B6916, Sigma) with bovine serum albumin (BSA; Sigma St. Louis, MO, USA) as the standard control. Proteins were stored at −80 °C for use in Western blotting.

Subcellular fractionation for Smurf2 protein localization

Subcellular fractionation from individual and pooled brains was performed as described in Sezgin et al., (2017) with minor modifications. Briefly, whole brain tissues and pooled brain regions were homogenized with Dounce homogenizer in 500 μL lysis buffer (50 mM Tris pH 7.5, 150 mM NaCl, %1 Triton X-100, 10 mM NaF and protease inhibitor [Roche, 5892970001]). Lysates were incubated on ice for 10 min and centrifuged at 14,000 rpm for 15 min at 4 °C. Supernatants were collected into a new tube as a cytosolic fraction and pellet including nuclear fraction were dissolved in 150 μL lysis RIPA buffer (50 mM Tris, pH 8.0, 150 mM NaCl, 1% NP40, 0.1% SDS and protease inhibitor [Roche, 5892970001]). The concentration of protein lysates was measured using the Bradford assay (B6916, Sigma) with bovine serum albumin (BSA; Sigma St. Louis, MO, USA) as the standard control. Proteins were stored at −80 °C for use in Western blotting.

Western blotting for Smurf2

From individual brain samples, 10 μg of protein lysate were loaded in the gel for the detection of Smurf2 and β-tubulin for young and old comparisons. From pooled brain regions, 20 μg of protein lysate were loaded in the gel for the detection of Smurf2 and β-tubulin for age and region comparison. For antibody validation, 100 μg of protein lysate from the embryonic zebrafish at 2, 3, and 4 dpf were loaded in the gel. From the cell lines 40 μg of protein lysate was loaded in the gel for the validation of the antibodies directed against Smurf2 due to the fact that they had never been tested previously in zebrafish tissues. For whole brain protein analysis, five biological replicates from each group (four groups: young female, young male, old female, and old male) were loaded in five cohorts at least three times, which also provided technical replicates, in a 10% resolving gel under reducing and denaturing conditions. For region-specific protein analysis, pooled brain samples were loaded at least three times in a 10% resolving gel under the same conditions. For protein analysis of subcellular fractions, three biological replicates of whole brain subcellular fractions from the two groups, young and old, were loaded in an 8% resolving gel under reducing and denaturing conditions at least three technical replicates.

At the same time, the subcellular fractions of pooled brain regions were loaded at least four times in an 8% resolving gel under the same conditions.

The Western blotting procedure was performed as described previously (Karoglu et al., 2017). Briefly, membranes were incubated in the following primary antibodies; anti-SMURF2, 200–300 aa, (ab94483, Abcam, Cambridge, UK, 1:2000 dilution in 5% milk solution), anti-SMURF2 C-terminal (ab211746, Abcam, 1:500 dilution in 5% milk solution), and anti-β-tubulin (CST #2146S, Cell Signaling Technology, Danvers, AM, USA, 1:5000 in 5% milk solution) as a loading control overnight at 4 °C. Secondary antibodies were goat-anti-rabbit IgG, HRP-linked antibody (CST #7074S, Cell Signaling Technology, 1:5000 dilution in 5% milk solution) for detecting the anti-SMURF2, 200–300 aa, (ab94483) antibody and the anti-β-tubulin, and goat-anti-mouse IgG-HRP antibody (sc-2005, Santa Cruz Biotechnology, Santa Cruz, CA, USA, 1:2500 dilution in 5% milk solution) for detecting the anti-SMURF2 C-terminal (ab211746) antibody. To validate the subcellular fractionation, anti-LaminB1 (66095-1-Ig, proteintech, 1:10,000 dilution in 5% milk solution, kindly provided from Dr. Sreeparna Banerjee's laboratory in Middle East Technical University), was utilized as a nuclear control while anti-β-tubulin (CST #2146S, Cell Signaling Technology, Danvers, AM, USA, 1:5000 in 5% milk solution) was used as a cytosolic control. The bands were detected with SuperSignal West Femto Maximum Sensitivity Substrate (34095, Thermo Fisher Scientific, Rockford, IL, USA) and the signal on membranes was visualized using a ChemiDoc MP Imaging System (Biorad, Hercules, CA, USA).

The band densities were quantified using the ImageJ program (NIH, Bethesda, MD, USA) and the author, ETK-E., who performed the quantification, was blind to the identity of the group to which the protein bands in the membrane belonged in order to achieve an unbiased quantification. For the analysis, we used tubulin (tub) normalization. The gel-normalized Smurf2 values were divided to gel-normalized values of the housekeeping control, β-tubulin, and values obtained with this calculation were designated as tub-normalized data.

RNA isolation

Individual and pooled snap-frozen brain samples were homogenized in TRIzol reagent (15596018, Invitrogen, Carlsbad, CA, USA) according to the manufacturer's instructions. The RNA concentration was measured with a NanoDrop 2000 machine (ThermoScientific), and then the TURBO DNA-free kit (AM1907, Invitrogen) was used to remove possible contamination from the DNA according to the manufacturer's instructions. The DNase-treated RNA concentration was measured with a NanoDrop 2000 machine (ThermoScientific).

Quantitative PCR (qRT-PCR)

All cDNAs were synthesized from 500 ng DNase-treated RNA samples by using an iScript cDNA Synthesis Kit (1708891, Biorad, Hercules, CA, USA). cDNA samples were diluted in a 1:4 or 1:8 ratio and 2 μL diluted cDNA was used for qPCR experiments. Reactions were performed in a 20 μL final volume. Light cycler 480 SYBR Green I Master mix solution (04887352001, Roche, Mannheim, Germany) was used according to the manufacturer's instructions. All qPCR experiments were done utilizing the Roche LightCycler 480 System. The primer sequences, and final primer concentrations are listed in Table 1.

STRING analysis for protein interacting partners of Smurf2

A protein network map of Smurf2 and its interacting partners, defined primarily by the literature, was analyzed for both humans and zebrafish using the STRING database (Szklarczyk et al., 2019). In the human interaction map, SMURF2, TP53, MDM2, YY1, EP300, SMAD7, and SIRT1 proteins were identified, while for the zebrafish map, smurf2, tp53, mdm2, yy1a, ep300a, smad7, and sirt1 proteins were defined. Due to the existence of teleost-specific gene duplication (Glasauer and Neuhauss, 2014), two paralogues of both ep300 and yy1 exist in the zebrafish genome and based on the literature (Shiu et al., 2016; Babu et al., 2018) only functional paralogues of ep300a and yy1a were accounted for in the current analysis. The minimum required interaction score was set to low confidence (0.150) because the default setting (medium confidence, 0.400) missed some interactions that have been verified in the literature such as that between Smurf2 and MDM2 (Nie et al., 2010).

qRT-PCR data analysis for Smurf2 and its interacting partners

ΔCt was calculated as Ct (target gene) – Ct (reference gene). *Rpl13a*, an internal control, was used as the

Table 1. Primer sequences used in the gene expression study

Gene symbol	Forward Primer 5′ –> 3′	Reverse Primer 5′ –> 3′	Final concentration in reaction
smurf2	ACTTCCTGCACACACAGACG	GGACCCAACTCCTCACAGTT	0.5 μM
tp53	TTGTCCCATATGAAGCACCACA	CAGCAACTGACCTTCCTGAGTC	0.5 μM
mdm2	GATTCGCGAAACGGTCAC	TCGTTGTCAACCTTGCTGAT	0.5 μM
smad7	CCCCTATGGGGTTTTCAGAT	GTGCCCTGAGGTAGGTCGTA	1 μM
yy1a	TGACAGGCAAGAAACTGCCA	TTGTGCAACCTTTGTGTGGG	1 μM
ep300a	GGCTTATGTGCCTATCTCCGA	GCCAAAATCGTTTCCATCGCT	1 μM
sirt1	TTCAGTGCCACGGGTCTTTT	GGACACCTGGGACAATGAGG	1 μM
rpl13a	TCTGGAGGACTGTAAGAGGTATGC	AGACGCACAATCTTGAGAGCAG	0.5 μM

reference gene (de Oliveira et al., 2014). ΔΔCt was calculated as the ΔCt of sample – average ΔCt of all samples and 2^(−ΔΔCt) was calculated to express fold changes. Finally, fold change values were $\log_2$ transformed to reduce the variation and get better visualization of the data for further statistical analysis.

Statistical analysis

The SPSS program (IBM, Armonk, NY, USA) was employed to perform statistical analysis of the gene and protein expression levels. Both datasets were tested for the assumptions of a normal distribution and homogeneity of variance with the Shapiro-Wilk and Levene tests, respectively. When these assumptions were violated, non-parametric tests including Mann-Whitney *U* test and Kruskal-Wallis test were applied. In the cases where the assumptions were fulfilled, parametric tests were applied. Specifically, for whole brain protein expression of both total lysates and subcellular fractions, an unpaired *t*-test was employed with the factor of age with the significance levels as $p < 0.05$. For region-specific protein expression of total lysates, because of the violation of assumptions, Kruskal-Wallis test was conducted between age and region followed by pairwise comparisons. Due to the fact that three pairwise comparisons were performed (Tel young vs. old, TeO young vs. old, Ce young vs. old), a Bonferroni-correction was applied and a new significance threshold of $p < 0.0167$ was used for these comparisons. However, a two-way ANOVA with factors of age and region was utilized to analyze subcellular fractions of region-specific protein expression levels. The gene expression levels in whole brain tissues were analyzed with a Mann-Whitney *U* test or an unpaired *t*-test. In the brain region-specific gene expression analysis, a two-way ANOVA was applied.

Further analysis of the gene expression levels in both the whole brain and the brain-specific regions was done using PCA with both the R (Free Software Foundation) and SPSS programs. Two principal components were extracted from the complete dataset of the expression levels of the seven genes with regard to the ΔCt values in order to determine the changes in each gene's amount relative to the others. A Pearson Correlation Matrix of the seven gene expression levels with respect to the ΔCt values was analyzed using the SPSS program to support the PCA. The graphic representations of both the gene and protein expression levels were generated using the SPSS program. The PCA plots were drawn with the prcomp method and the fviz_pca_biplot package in R.

RESULTS

Western blot validation of Smurf2 antibodies

Previous results from our laboratory demonstrated that gene expression levels of *smurf2* increase in the aged zebrafish brain (Arslan-Ergul and Adams, 2014). Thus, our initial hypothesis was that the protein expression levels of Smurf2 would parallel this observed increase in mRNA levels during brain aging. To achieve this goal, we used Western blot analysis to measure Smurf2 protein levels, and prior to this, we validated two commercially-available anti-SMURF2 antibodies, which had not been used previously in zebrafish tissues. The first antibody we used was an anti-SMURF2, 200–300 aa, from Abcam (Abcam, ab94483, Cambridge, UK), which recognizes the 200–300 amino acid residues of the human SMURF2 protein. The blot yielded the expected Smurf2 protein band at the 86 kDa molecular weight in all the samples of the cell line lysates, as well as lysates from zebrafish embryos and larvae at 2, 3 and 4 days post fertilization (dpf; Fig. 1A). Using a well-characterized antibody for zebrafish tissues, the expected α-β-tubulin band (55 kDa) was also observed in the Western blot procedure (Fig. 1A). Moreover, young and old zebrafish brain lysates, which were blotted with the anti-SMURF2, 200–300 aa, antibody, yielded the expected 86 kDa Smurf2 protein band. Thus, our initial experiments validated the anti-SMURF2, 200–300 aa, antibody for use in both zebrafish larvae and the adult brain (Fig. 1A).

A second antibody from Abcam (anti-SMURF2 C-terminal, ab211746, Abcam, Cambridge, UK) directed against the human SMURF2 C-terminal region was utilized and validated for use in zebrafish tissues. All the cell line lysates, more specifically the breast cancer cell line, MDA-MB-231, which is the positive control for the anti-SMURF2 C-terminal antibody, produced the expected 86 kDa band in the immunoblots (Fig. 1A). To our surprise and interest, embryos and larvae at the 2–4 dpf stages had a band of approximately 100 kDa, which is slightly larger than the expected band observed in the cell line lysates. Moreover, when we blotted the membrane that contained young and old zebrafish brain lysates, with the anti-SMURF2 C-terminal antibody, an even larger Smurf2 band at the molecular weight of 250 kDa, not the expected 86 kDa protein, was detected (Fig. 1A). These differences in the molecular weights of the specific bands in zebrafish brain tissue lysates as compared to zebrafish embryos and larvae at 2–4 dpf, as well as the cell line lysates, might point to possible regulatory mechanisms such as PTMs on the Smurf2 protein or the formation of a complex between this protein and its interacting partners that begins to occur during embryonic development and continues into later stages of brain aging.

Smurf2 gene expression increases in a region-specific manner during brain aging

We hypothesized that the protein levels of Smurf2 would change in the same direction as the gene expression levels. To test our hypothesis that the protein levels of Smurf2 increase in the brain with age, we performed Western blot analysis in young and old zebrafish brain tissues using the two different commercially-available antibodies that were validated by us. Moreover, in order to examine any region-specific alterations in Smurf2 protein levels, three brain areas including the telencephalon (Tel), the optic tectum (TeO) and the cerebellum/medulla/spinal cord (Ce) were microdissected from the whole zebrafish brains of young and old

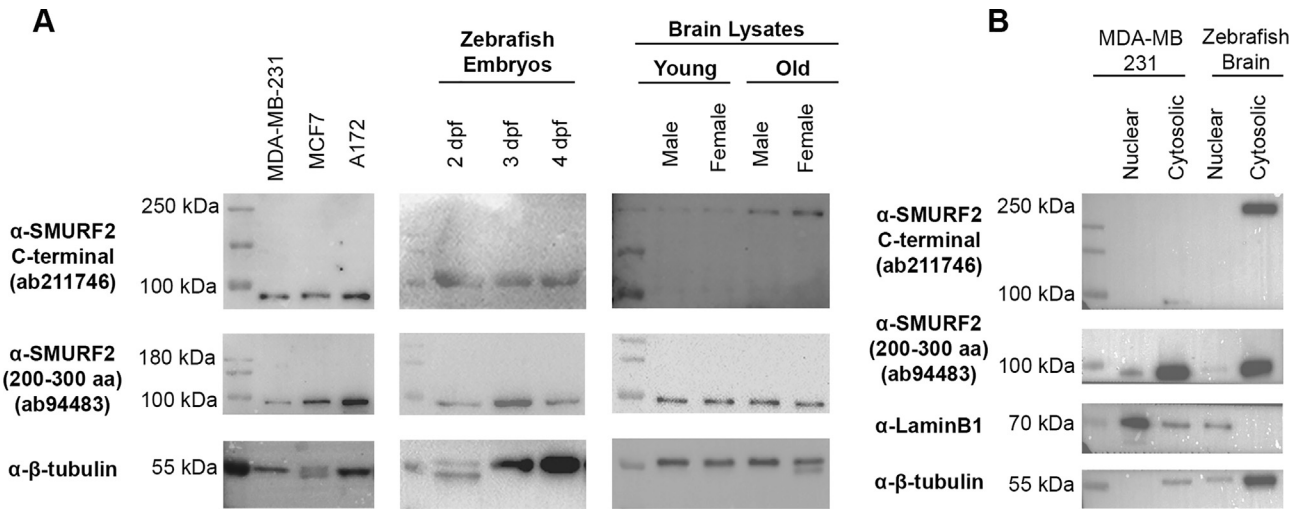

Fig. 1. Antibody validation of anti-SMURF2 antibodies, the anti-SMURF2, 200–300 aa, and anti-SMURF2 C-terminal antibody. **(A)** Protein lysates from the MDA-MB-231 cell line, which is the positive control for the anti-SMURF2 C-terminal antibody, and the MCF7 cell line, which is the positive control for the anti-SMURF2, 200–300 aa, antibody, and the A172 cell line used as a control for brain cells, gave the expected molecular weight of 86 kDa in the immunoblot using both of the anti-SMURF2 antibodies. Protein lysates of zebrafish embryos and larvae at 2, 3 and 4 dpf gave the expected band in the immunoblot using anti-SMURF2, 200–300 aa, antibody, and the expected band with a small shift in the molecular weight to approximately 100 kDa in the immunoblot with the anti-SMURF2 C-terminal antibody. The anti-SMURF2 C-terminal antibody recognized an even larger band of approximately 250 kDa in young and old zebrafish brains, as well as the expected molecular weight band of 86 kDa with the anti-SMURF2, 200–300 aa, antibody. **(B)** Subcellular fractionation was validated with a nuclear marker, LaminB1 and a cytosolic marker, β-tubulin.

animals (Fig. 2A). While cerebellum, medulla and spinal cord are evolutionary and functionally distinct regions, we pooled them in our analysis since it is technically difficult to remove regions. Our aim was to separate three integrative centers as Tel, TeO and Ce as defined in Wullimann et al. (1996). Also, our main focus was the changes in Tel region because Tel is more prominent region in respect to cognitive functions. Previous detailed molecular analysis demonstrated that different parts of Tel have roles not only in the control of sensory and motor functions but also in cognitive tasks including learning and memory (Ganz et al., 2014). Moreover, the putative homologues of mammalian hippocampus and amygdala were already defined in the zebrafish Tel region as the ventral division of the lateral zone of area dorsalis (Dlv in medial pallium) and the medial zone of the dorsal telencephalic area (Dm in ventral pallium), respectively (Ganz et al., 2014). Several studies demonstrated that long-term potentiation (LTP), which is the cellular basis of synaptic plasticity underlying learning and memory, occurs in the Tel region of zebrafish brain (Nam et al., 2004; Ng et al., 2012; Wu et al., 2017). More importantly, although the zebrafish brain has 16 distinct zones of neurogenesis, which is not restricted to the telencephalon, but is widespread throughout the entire brain (Grandel et al., 2006; Kizil et al., 2012), neurogenesis decreases with advancing age in the Tel (Edelmann et al., 2013; Arslan-Ergul et al., 2016).

Initially the anti-SMURF2, 200–300 aa, antibody recognizing the region between the 200–300 amino acid residues of the human SMURF2 protein was used. Young and old zebrafish brain protein samples were loaded in the gel and this was repeated at least three times, and then the protein levels of Smurf2 were determined by blotting with the anti-SMURF2, 200–300 aa, antibody, along with the housekeeping control antibody, anti-β-tubulin. Both proteins were quantified followed by tub-normalization. According to an independent sample *t*-test, there was no significant effect of age on the whole brain protein levels of tub-normalized Smurf2 ($t(18) = 1.059$, $p = 0.304$, Fig. 2B). However, a region-specific analysis indicated that Smurf2 protein levels changed significantly and there was an interaction between age and region groups ($\chi^2(5) = 11.990$, $p = 0.035$) and pairwise comparisons showed that Smurf2 protein increased significantly during aging in the Tel ($p = 0.003$) but not in TeO ($p = 0.726$) and Ce ($p = 0.121$) areas (Fig. 2B).

The second antibody recognizing the C-terminal region of the SMURF2 protein was used subsequently in order to test whether the protein levels detected with the anti-SMURF2 C-terminal antibody changed in the aged brain. To accomplish this, the same protein samples were loaded again using SDS-PAGE and this time blotted with the anti-SMURF2 C-terminal antibody, as well as anti-β-tubulin. Interestingly, the band recognized by this anti-SMURF2 C-terminal antibody directed against Smurf2 was larger, with a weight of approximately 250 kDa not the expected molecular weight of 86 kDa (Fig. 1A). The bands in the blots were quantified and tub-normalized to test our hypothesis as to whether or not Smurf2 levels change during brain aging. There was no significant main effect of age on tub-normalized Smurf2 levels ($t(18) = -1.046$, $p = 0.309$, Fig. 2C) although there was a numerical increase with age. Moreover, in a manner similar to the data using the anti-SMURF2, 200–300 aa, antibody, the anti-SMURF2 C-terminal antibody showed significant changes between age and region ($\chi^2(5) = 17.275$, $p = 0.004$) and a region-specific significant increase

with advancing age in the Tel ($p = 0.002$) and Ce ($p = 0.008$) but not in the TeO ($p = 0.703$) areas (Fig. 2C). Since we observed increases in Smurf2 protein levels that are brain-region selective, we concluded that any changes in *smurf2* mRNA levels are not leading to global brain alterations. Moreover, due to the fact that in the Ce brain area protein levels are not similar using the two different antibodies, this may represent PTMs in the Smurf2 protein that are increasing during brain aging. The other possibility we considered is that the complex formation of Smurf2 with other proteins such as Smad7 and TGF-β receptors, may increase molecular weight.

Subcellular localization of Smurf2 is mostly cytosolic in zebrafish brain

Research has determined a role for the Smurf2-Smad7 complex in degrading the TGF-β receptor complex in the cytosol (Kavsak et al., 2000) or in targeting substrates for ubiquitin-mediated degradation in the nucleus (Wiesner et al., 2007). To determine any effects of age on the subcellular localization of Smurf2 or Smurf2 complex structure, we performed fractionation experiments to analyze nuclear and cytosolic fractions separately across different groups. Firstly, we validated the subcellular fractionation method with nuclear marker, LaminB1, and cytosolic marker, β-tubulin (Fig. 1B). Both fractions of each sample were loaded on the gel at least three times and the immunoblots of both individual whole brain and pooled brain regions (Fig. 3A) indicated that Smurf2 protein recognized by both antibodies was mostly detected in cytosolic fraction. The increased molecular weight of Smurf2 protein recognized by anti-SMURF2 C-terminal antibody was also present and enriched in the cytosolic fraction; it implied that this antibody might recognize the complex of Smurf2 in the cytosol while the anti-SMURF2, 200–300 aa, antibody binds to cytosolic Smuf2 but not in a complex structure (86 kDa).

Fractionation experiments performed in the whole brain of young and old animals (Fig. 3) showed similar results with those done in total lysates (Fig. 2B, C). The pattern demonstrated that tub-normalized Smurf2 protein increased but was not statistically significant for both the anti-SMURF2, 200–300 aa, antibody ($t(4) = -0.470$, $p = 0.663$) and anti-SMURF2 C-terminal antibody ($t(4) = -0.632$, $p = 0.562$). Region-specific analysis of the anti-SMURF2 C-terminal antibody showed that both the main effect of age was close to being statistically significant ($F_{(1,24)} = 3.977$, $p = 0.058$, Fig. 3B) and the main effect of region was also close to being statistically significant ($F_{(2,24)} = 3.356$, $p = 0.052$). However, the interaction effect of age by region was not significantly different ($F_{(2,24)} = 0.718$, $p = 0.498$, Fig. 3C). Moreover, Smurf2 expression recognized by the anti-SMURF2, 200–300 aa, was statistically significant in terms of the main effect of region ($F_{(2,22)} = 7.512$, $p = 0.003$) while the main effect of age ($F_{(1,22)} = 1.714$, $p = 0.204$) and the interaction effect between age and region ($F_{(2,22)} = 0.276$, $p = 0.761$, Fig. 3D) was not statistically different. The similar results in Smurf2 protein levels changes observed between the experiments using total protein extract and subcellular fractionation along with the anti-SMURF2 C-terminal

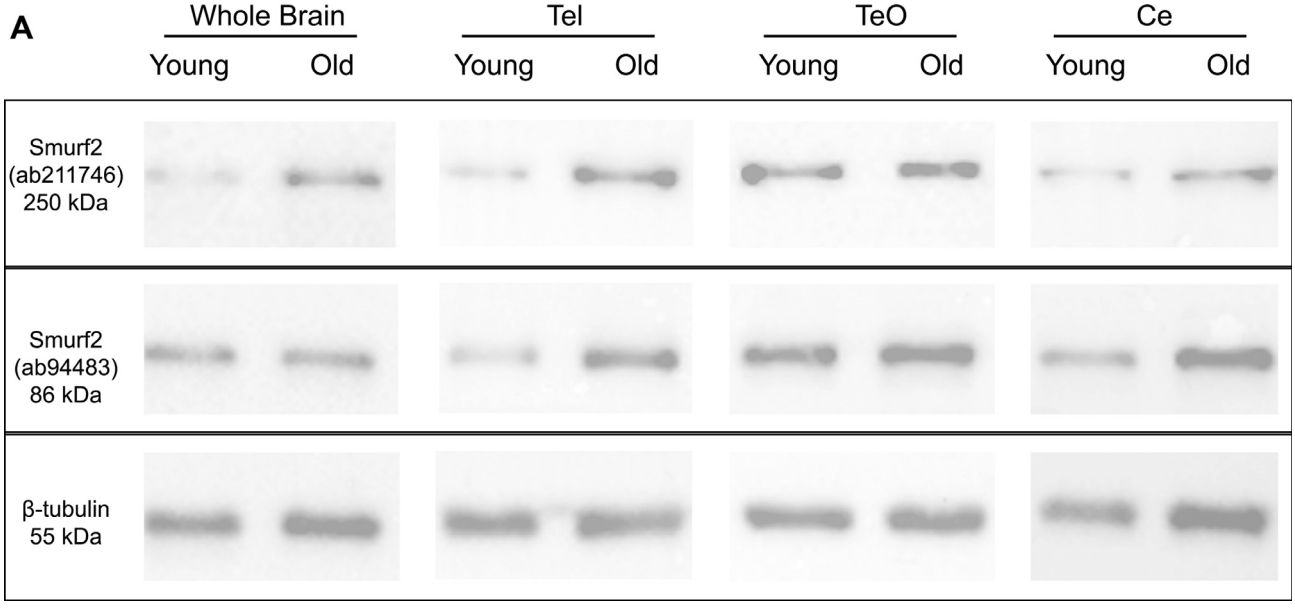

Fig. 2. Smurf2 protein levels were altered in a region-specific manner during brain aging. **(A)** Representative Western blots for both Smurf2 and the β-tubulin antibodies in the individual whole brains of young and old zebrafish and the brain-specific regions of young and old zebrafish, including the telencephalon (Tel), the optic tectum (TeO) and the cerebellum/medulla/spinal cord (Ce) areas. **(B)** Smurf2 protein expression levels detected with the anti-SMURF2 (200–300 aa) antibody, directed against the internal 200–300 amino acid residues, did not change with age in the whole brain, TeO and Ce regions, whereas they increased significantly with age in the Tel. **(C)** Smurf2 protein expression levels detected with the anti-SMURF2 C-terminal antibody, directed against the C-terminal region, increased numerically but not statistically in the whole brain and TeO areas, while in Tel and Ce, the levels were significantly higher in the old brain lysates as compared to those of the young animals. Tub-normalized values are indicated in **(B)** and **(C)**. Data are represented as boxplots and * indicates $p < 0.0167$.

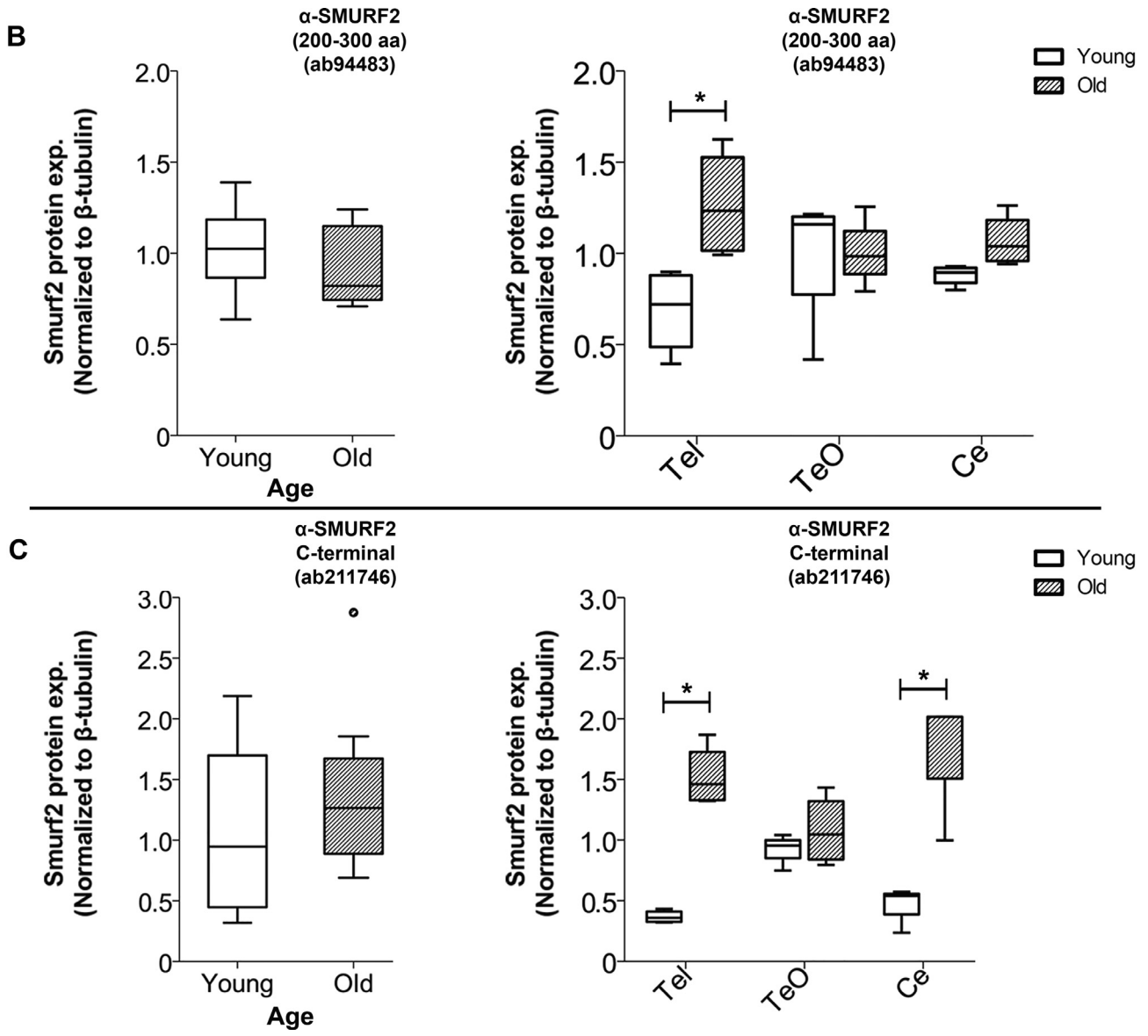

Fig. 2 (*continued*)

antibody likely indicates that the contribution of cytosolic fraction not the nuclear was driving the changes in the total lysates.

Identification of interacting partners of SMURF2 using computational analysis for biological determination of differential expression patterns in the aged brain

Since the interacting and downstream partners work with Smurf2 in several cellular processes, their gene expression levels were also analyzed to determine whether alterations exist during brain aging. Due to the fact that the gene expression levels of *smurf2* increase in the aged brain (Arslan-Ergul and Adams, 2014), we hypothesized that some interacting partners and downstream genes would also be affected by the upregulation of *smurf2* with age. The transcription factor, tp53, responds to several factors that induce cellular stress by regulating target genes, which promote growth arrest, DNA repair, cellular senescence, and apoptosis (Li et al., 2002a). Based on the literature, tp53 is an indirect target of Smurf2, which degrades YY1 (Jeong et al., 2014) and/or stabilizes MDM2 (Nie et al., 2010). YY1 is a target of Smurf2 that is regulated by proteasome-mediated degradation, and the degradation of YY1 by Smurf2 relieves the suppression of tp53 activity (Jeong et al., 2014). Similarly, MDM2, a ubiquitin ligase, is a negative regulator of tp53 and its stability is maintained by Smurf2 (Nie et al., 2010). On the other hand, Smad7 is an adaptor protein that recruits both Smurf2 to the TGF-β receptor complex, as well as Smad7 itself, for ubiquitin-mediated proteasomal degradation. Additionally, Smad7 interaction leads to the export of Smurf2 from the nucleus to the cytosol (Kavsak et al., 2000; Yan et al., 2009). Smad7 is acetylated by ep300, and stabilized by

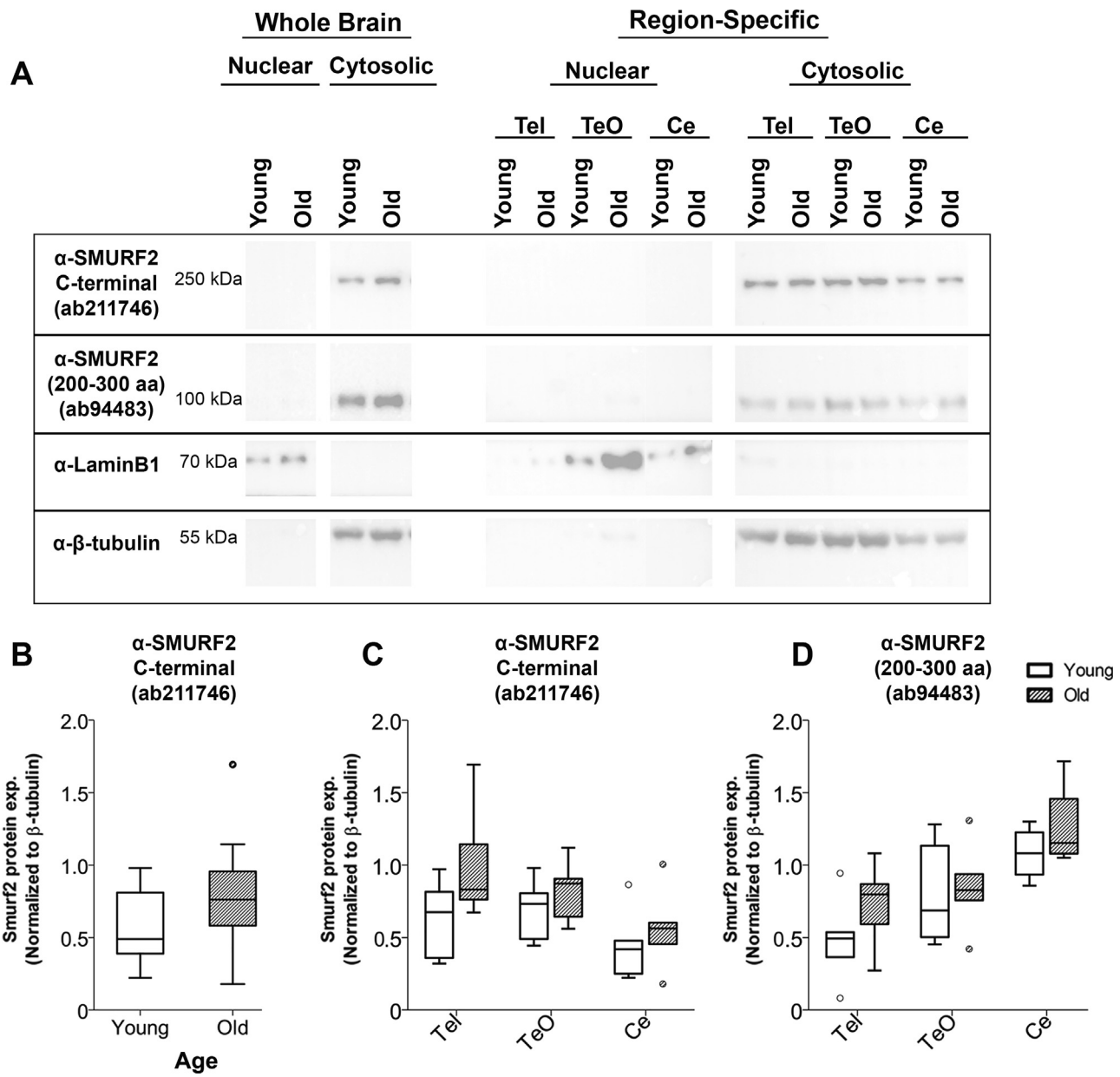

Fig. 3. Smurf2 protein was enriched in the cytosolic fraction of the zebrafish brain. Representative Western blots for both Smurf2, LaminB1 and the β-tubulin antibodies in the nuclear and cytosolic fractions of **(A)** individual whole brains of young and old zebrafish and the brain-specific regions of young and old zebrafish, including the telencephalon (Tel), the optic tectum (TeO) and the cerebellum/medulla/spinal cord (Ce) areas. Smurf2 protein expression levels detected with the anti-SMURF2 C-terminal antibody increased with advancing age **(B)** and increased in old Tel **(C)** as compared to young in region-specific analysis. **(D)** Smurf2 protein expression levels detected with the anti-SMURF2, 200–300 aa, antibody did not change significantly with age. Tub-normalized values are indicated in **(B)**, **(C)** and **(D)**. Data are represented as boxplots.

protecting against Smurf2-ubiquitination (Grönroos et al., 2002; Simonsson et al., 2005). Moreover, ep300 acetylates tp53 during stress responses but MDM2 suppresses the ep300-mediated tp53 acetylation (Ito et al., 2001). SIRT1 is also one of the Smad7-binding partners and deacetylates Smad7 and inhibits TGF-β signaling (Yan et al., 2009). All of the interacting partners and substrates of Smurf2 chosen for analysis in the current study (Fig. 4) were done and their interaction scores were obtained from STRING database (Table 2) because they have intricate functional relationships with each other, as well as having regulatory roles in cellular senescence.

Although there is a 70% homology of the zebrafish genome with the human (Howe et al., 2013), some candidate genes in zebrafish have 2 paralogues because of the teleost specific gene duplication (Glasauer and Neuhauss, 2014). For example, there are 2 paralogues of *ep300*; *ep300a*, and *ep300b*. Based on the study of Babu et al. (2018), the expression of both *ep300a* and *ep300b* at 4 dpf larvae was more specific to the brain

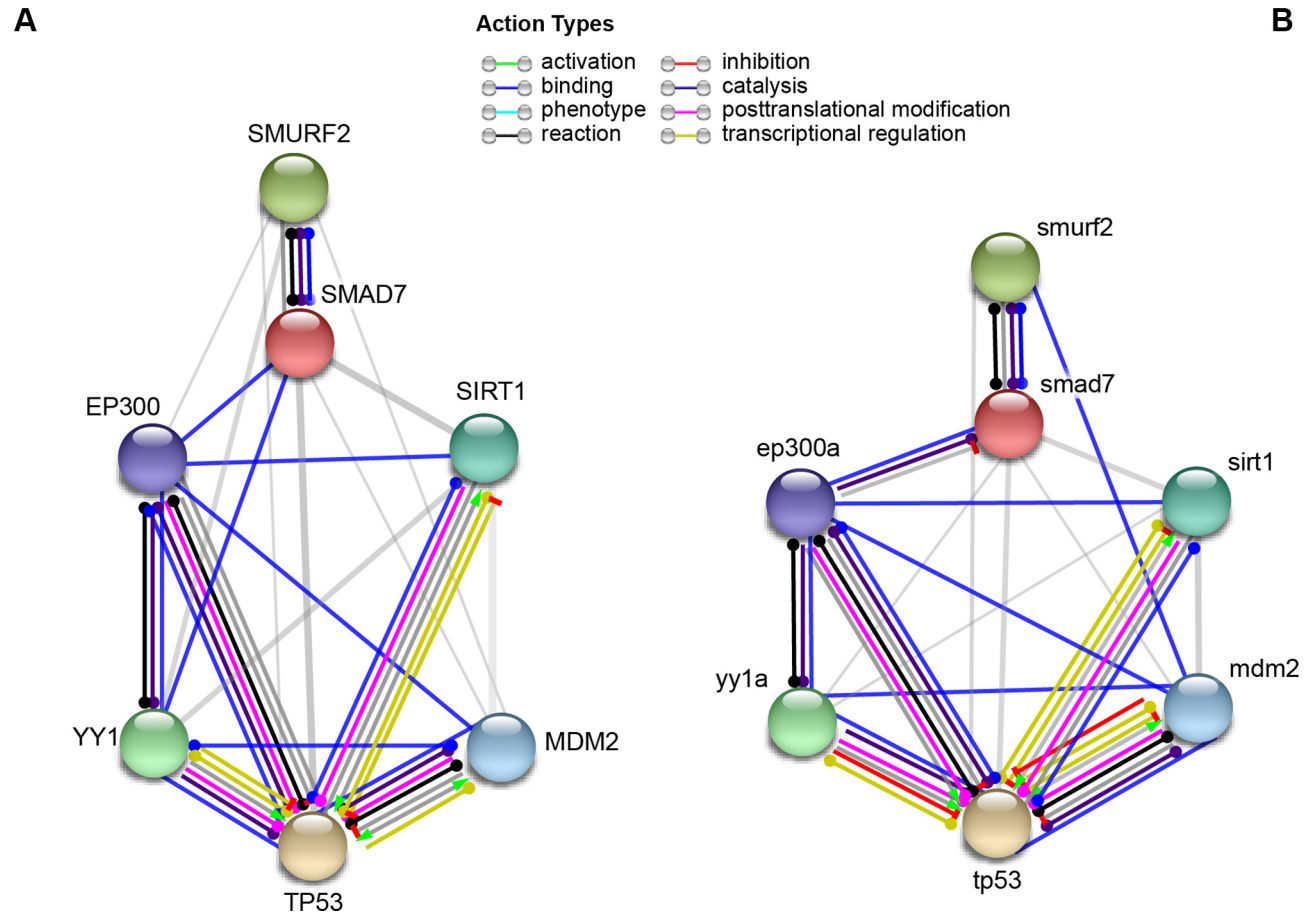

Fig. 4. STRING analysis of 7 proteins in **(A)** human; **(B)** zebrafish. Color nodes represent the proteins and color lines represent interaction type between nodes. Green line: activation, red line: inhibition, blue line: binding, purple line: catalysis, cyan line: phenotype, magenta line: PTM, black line: reaction, yellow line: transcriptional regulation. (For interpretation of the references to colour in this figure legend, the reader is referred to the web version of this article.)

Table 2. Interaction scores of proteins of interest in (A) Human and (B) Zebrafish. Provided from STRING database

A-Human			B-Zebrafish		
node1	node2	combined_score	node1	node2	combined_score
TP53	MDM2	0.999	mdm2	tp53	0.999
TP53	EP300	0.999	smurf2	smad7	0.994
SMURF2	SMAD7	0.997	sirt1	tp53	0.992
TP53	SIRT1	0.996	ep300a	tp53	0.992
EP300	SIRT1	0.994	ep300a	sirt1	0.788
TP53	YY1	0.987	yy1a	tp53	0.730
EP300	YY1	0.975	mdm2	sirt1	0.575
EP300	MDM2	0.975	sirt1	smad7	0.515
YY1	MDM2	0.956	ep300a	mdm2	0.507
MDM2	SIRT1	0.703	tp53	smad7	0.488
EP300	SMAD7	0.682	ep300a	smad7	0.428
TP53	SMAD7	0.650	ep300a	yy1a	0.424
SMAD7	SIRT1	0.648	sirt1	yy1a	0.394
YY1	SIRT1	0.527	mdm2	yy1a	0.327
YY1	SMAD7	0.516	yy1a	smad7	0.306
SMURF2	YY1	0.485	smurf2	tp53	0.260
TP53	SMURF2	0.316	mdm2	smurf2	0.240
SMURF2	MDM2	0.300	mdm2	smad7	0.232
SMAD7	MDM2	0.295	ep300a	smurf2	0.182
EP300	SMURF2	0.259	yy1a	smurf2	0.158

region, and the expression of *ep300a* and *ep300b* had the highest level in the brain among all adult tissues. However, ep300a is a catalytically active acetyltransferase in the brain while ep300b is not active in the brain (Babu et al., 2018). In addition to *ep300*, *yy1* has 2 paralogues as *yy1a* and *yy1b*. At the 3 dpf larval stage, *yy1a* expression was detected in the brain and eye. Knockdown of *yy1a* using the antisense morpholino technique caused an increase in *tp53* and shrinking of the developing mid- and hindbrains in 3dpf *yy1a* morphants as compared to control embryos (Shiu et al., 2016). For these reasons, *ep300a* and *yy1a*, the functional paralogues of the human genes, and the other five genes with only one paralogue, *smurf2*, *mdm2*, *tp53*, *smad7*, and *sirt1*, were used in the STRING database analysis and the subsequent gene expression analyses with qRT-PCR.

As seen in Fig. 4, in both humans and zebrafish, Smurf2 and all of its functional partners analyzed had protein–protein interactions that control binding, catalysis, activation, inhibition, as well as post-translational and transcriptional regulation. The STRING database analysis indicated that SMURF2 and SMAD7 affect each other with respect to binding, reaction, and catalysis, and inhibition in humans and zebrafish. Moreover, SMURF2 interacts with YY1, EP300, TP53, and MDM2 in humans. However, it was demonstrated that Smurf2 has relationships only with smad7, tp53, and mdm2 in zebrafish. Interactions indicated with a gray color line means that two proteins are functionally associated based on the STRING score, but the type of interaction is as yet unknown. However, the relationships between YY1 and TP53 as well as MDM2 and TP53 are well described in terms of the binding, PTMs, transcriptional regulation, and inhibition. EP300 in humans and ep300a in zebrafish both have binding interactions with SMAD7, SIRT1, MDM2, YY1, and TP53, and thus it would suggest that EP300 is a regulator of the proteins of interest that have a role in aging. Since the proteins of these genes strongly interact, it supports our aim of analyzing the gene expression levels of *smad7*, *tp53*, *mdm2*, *yy1a*, *ep300a*, and *sirt1* in addition to *smurf2*.

The gene expression levels of Smurf2 and its interacting partners are differentially altered in the whole brain and brain-specific regions during aging

The gene expression patterns of the following genes, including *smurf2*, *tp53*, *mdm2*, *ep300a*, *yy1a*, *smad7*, and *sirt1*, were analyzed using qRT-PCR in the whole brains of the young and old animals. As shown in Fig. 5A, *smurf2* gene expression levels increased significantly with old age ($U = 5.00$, $z = -2.082$, $p = 0.037$). It was observed that the expression levels of *mdm2* and *yy1a* numerically increased in the aged brain although this upregulation was not statistically significant, and this is likely due to a large variance ($U = 8.00$, $z = -1.061$, $p = 0.109$ *mdm2;* $U = 11.00$, $z = -1.121$, $p = 0.262$ *yy1a*). Similarly, *ep300a* and *sirt1* had an increase in their expression levels in old brains but there were no significant differences between the age groups ($t(10) = -1.561$, $p = 0.149$ *ep300a;* $U = 10.00$, $z = -1.281$, $p = 0.200$ *sirt1*). Furthermore, *tp53* and *smad7* were stable during brain aging ($t(10) = -0.447$, $p = 0.665$ *tp53*; $t(10) = -0.138$, $p = 0.893$ *smad7*; Fig. 5A). Since the aforementioned genes of interest have roles in transcriptional and translational regulations such as ubiquitination, acetylation, and deacetylation and functionally affect each other, a compensation mechanism may be occurring in their gene expression levels during brain aging. Several studies have shown that PTMs compete with each other to regulate the stability of common targets such as tp53 and Smad7, or one PTM may either promote or prevent the further modification on the proteins targeted by other PTMs (Grönroos et al., 2002; Li et al., 2002a; Brooks and Gu, 2003; Simonsson et al., 2005). In the current study, Smurf2 and its interacting partners, with the exception of Smad7 and tp53, increased with age. Therefore, increased gene expression levels in one of the target genes might trigger the upregulation of the other 4 genes to eliminate a bias towards a specific PTM. For example, in the presence of ep300, the amount of Smad7 was significantly increased because the acetylation of Smad7 prevented its ubiquitination and subsequent degradation (Grönroos et al., 2002). Thus, any shift in the balance between PTMs might trigger the activation of other PTM mechanisms to stabilize the cell again.

Since we observed that there is brain region-specific regulation in the protein expression levels of Smurf2, we tested the hypothesis that gene expression levels of Smurf2 and its interacting partners may be regulated in a similar manner. To test this possibility, we performed qRT-PCR analysis for the seven genes of interest of the pooled brain regions, which included Tel, TeO and Ce. According to the results of a two-way ANOVA, there were a significant main effects of age ($F_{(1,18)} = 54.251$, $p < 0.0005$) and region ($F_{(2,18)} = 6.072$, $p = 0.010$) on *smurf2* gene expression levels. More importantly, there was a significant interaction between age and region ($F_{(2,18)} = 34.059$, $p < 0.0005$) on *smurf2* levels. Pairwise comparisons indicated that a significant effect of age in both Tel ($p < 0.0005$) and Ce ($p = 0.013$). Additionally, there was a significant effect of region in both young (Tel vs. TeO $p < 0.0005$, Tel vs. Ce $p = 0.014$ and TeO vs. Ce $p = 0.002$) and old (Tel vs. TeO $p = 0.002$, Tel vs. Ce $p = 0.001$) groups (Fig. 5B). While *smurf2* expression levels in the whole brain increased significantly during aging (Fig. 5A), the region-specific expression levels in Tel and Ce decreased with age (Fig. 5B). Not surprisingly, there was no significant main effect of age on *tp53* ($F_{(1,18)} = 1.297$, $p = 0.270$, Fig. 5C), *yy1a* ($F_{(1,18)} = 0.012$, $p = 0.914$, Fig. 5F) and *smad7* ($F_{(1,18)} = 1.235$, $p = 0.281$, Fig. 5G) levels which was in a manner similar to their expression in the whole zebrafish brain (Fig. 5A). Similarly, there was neither a significant main effect of region on *tp53* ($F_{(2,18)} = 0.131$, $p = 0.878$, Fig. 5C), *yy1a* ($F_{(2,18)} = 2.035$, $p = 0.160$, Fig. 5F) and *smad7* ($F_{(2,18)} = 2.720$, $p = 0.093$, Fig. 5G) nor a significant interaction between age and region on *tp53* ($F_{(2,18)} = 1.328$, $p = 0.290$, Fig. 5C), *yy1a* ($F_{(2,18)} = 1.047$, $p = 0.371$, Fig. 5F) and *smad7*

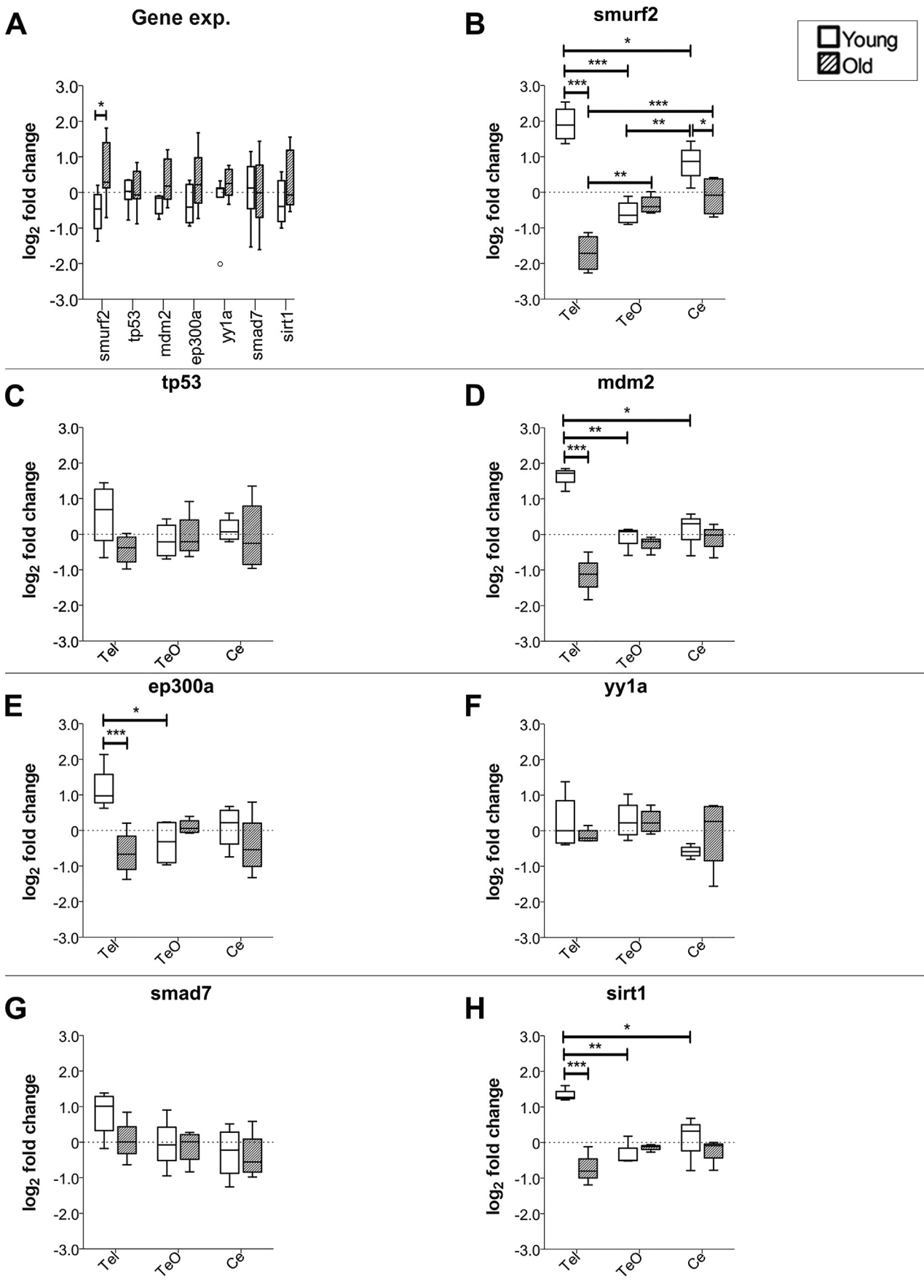
A
Gene exp.
log2 fold change
smurf2
tp53
mdm2
ep300a
yy1a
smad7
sirt1
B
smurf2
Young
Old
Tel
TeO
Ce
C
tp53
D
mdm2
E
ep300a
F
yy1a
G
smad7
H
sirt1

($F_{(2,18)}$ = 0.657, p = 0.530, Fig. 5G). However, analysis of *mdm2* indicated that its expression levels were altered significantly with age ($F_{(1,12)}$ = 21.003, p = 0.001, Fig. 5D) but not by region ($F_{(2,12)}$ = 1.166, p = 0.344). Nevertheless, there was a statistically significant interaction between age and region on *mdm2* expression levels ($F_{(2,12)}$ = 13.953, p = 0.001). Pairwise comparisons revealed that there was a significant main effect of age in Tel (p < 0.0005) and region in the young group (Tel vs. TeO p = 0.003 and Tel vs. Ce p = 0.007, Fig. 5D). Moreover, *ep300a* expression levels were altered significantly with respect to factor of age ($F_{(1,18)}$ = 5.419, p = 0.032, Fig. 5E) and there was an age by region interaction ($F_{(2,18)}$ = 6.092, p = 0.010). There was a significant main effect of age in the Tel (p = 0.001) and region in the young group (Tel vs. TeO p = 0.012) on *ep300a* expression levels. In a similar manner, there was a significant main effect of age ($F_{(1,12)}$ = 12.305, p = 0.004, Fig. 5H) and an age by region interaction ($F_{(2,12)}$ = 9.299, p = 0.004) on *sirt1* levels. These effects on *sirt1* levels were driven by age in the Tel (p < 0.0005) and region in young animals (Tel vs. TeO p = 0.003 and Tel vs. Ce p = 0.015, Fig. 5H). However, there were no significant main effects of region on both *ep300a* ($F_{(2,18)}$ = 1.072, p = 0.362) and *sirt1* ($F_{(2,12)}$ = 2.323, p = 0.140) expression levels.

Multivariate analysis of gene expression levels in the brain demonstrates a potential balance between ubiquitination, acetylation, and deacetylation during aging

In order to determine alterations in the expression levels of each gene as compared to the others, further investigation of their levels was done using PCA. In the complete dataset, which included the gene expression levels of the seven selected target genes with regards to ΔCt values, two components were extracted independent of the factor of age. The first component (PC1) explained 75.3% of the variance in the data and PC1 was driven by all seven genes because of their component loading values, which were greater than 0.5. The second component (PC2) contributed to 11.2% of the variance in the dataset and was influenced by only *yy1a* (component loading score > 0.5) and marginally affected by *mdm2* (component loading score = 0.427). Moreover, the correlation matrix in Table 3 indicated that there was neither a correlation between *yy1a* and *mdm2* nor one between *yy1a* and *tp53*, whereas the other genes were correlated with each other. It was also predicted from the loading plot in Fig. 6 that *yy1a* and *mdm2* had an inverse contribution to the overall covariance. The correlation matrix (Table 3) also indicated that *smad7* was correlated with neither *tp53* nor *mdm2* in whole zebrafish brain as suggested from their inverse contribution in the loading plot (Fig. 6). Moreover, the loading plot demonstrated that *smurf2*, *sirt1*, and *ep300a* contributed to the variance in the same way, and this was also evident in the correlation matrix that demonstrated a significantly higher correlation between *smurf2*, *ep300a*, and *sirt1* (Pearson correlation > 0.9; Table 3). These three genes have roles in regulating similar targets, such as tp53 and smad7, via different pathways, which could increase the likelihood of PTMs, ubiquitination, acetylation, and deacetylation. As seen in the scatterplot in Fig. 6 the data might indicate that the factor of age has a differential impact on the variance. The data demonstrated that PC2 did not majorly affect the variance in the old group, whereas it has an apparent contribution to that seen in the young group (Fig. 6). Also, in the young group, only *smurf2*, *ep300a*, and *sirt1* were associated with each other significantly, while in the old group almost all genes were correlated (data not shown). It may indicate that the balance between ubiquitination, acetylation, and deacetylation mediated by Smurf2, ep300a, and Sirt1 is enough to maintain the stability of target proteins, however during brain aging there may be a shift and other factors take a role to maintain cell stability. From this data, it is possible to infer that *smurf2* as well as *ep300a*, and *sirt1* have regulatory roles during brain aging because of their position in controlling PTMs.

To examine the region-specific alterations of gene expression patterns as compared to each one of the others, further analysis was conducted with PCA. In the region-specific dataset, which included the expression levels of 7 selected target genes in pooled young-old zebrafish brain regions either in the Tel, TeO or Ce measured by the ΔCt values, two components were extracted independently of the factor of age. The first component (PC1) explained 79.5%, 58.9%, and 78.8 % of the total variance in Tel, TeO and Ce dataset, respectively and PC1 of all three regions were driven by all seven genes. However, the second component (PC2) of each region had different contribution to the genes of interest. For the Tel specific dataset (Fig. 7A), PC2 contributed to 11.2% of the variance and was influenced only by *yy1a* (component loading score > 0.5). Moreover, in the Ce dataset (Fig. 7C), PC2 contributed to 16.1% of the variance and was driven by *yy1a* and marginally by *tp53* and *sirt1*. However, in the TeO region (Fig. 7B), PC2 had a 30.6% contribution to the variance and this was driven by *smurf2*, *smad7*, and *sirt1* as well as *yy1a*. Moreover, the correlation matrices of the region-specific gene expression (Tables 4–6) showed different patterns in each region. Noticeably, TeO-specific expression had a distinct correlation between *yy1a* and *mdm2* (Table 5), whereas neither the whole brain analysis (Table 3) nor the Tel- or Ce-specific region analysis (Tables 4 and 6) demonstrated

Fig. 5. The relative gene expression levels of *smurf2* and its interacting partners illustrated by age and region. **(A)** The relative expression levels of the target genes of interest in whole zebrafish brain during aging. The brain region-specific expression levels of **(B)** *smurf2*, **(C)** *tp53*, **(D)** *mdm2*, **(E)** *ep300a*, **(F)** *yy1a*, **(G)** *smad7* and **(H)** *sirt1* during aging. Data are represented as boxplots and * indicates p < 0.05, ** indicates p < 0.01, *** indicates p < 0.001.

Table 3. Correlation matrix of target genes of interest in whole zebrafish brain. Significance of correlation coefficients (2-tailed): *$p < 0.05$, **$p < 0.01$. ($n = 12$)

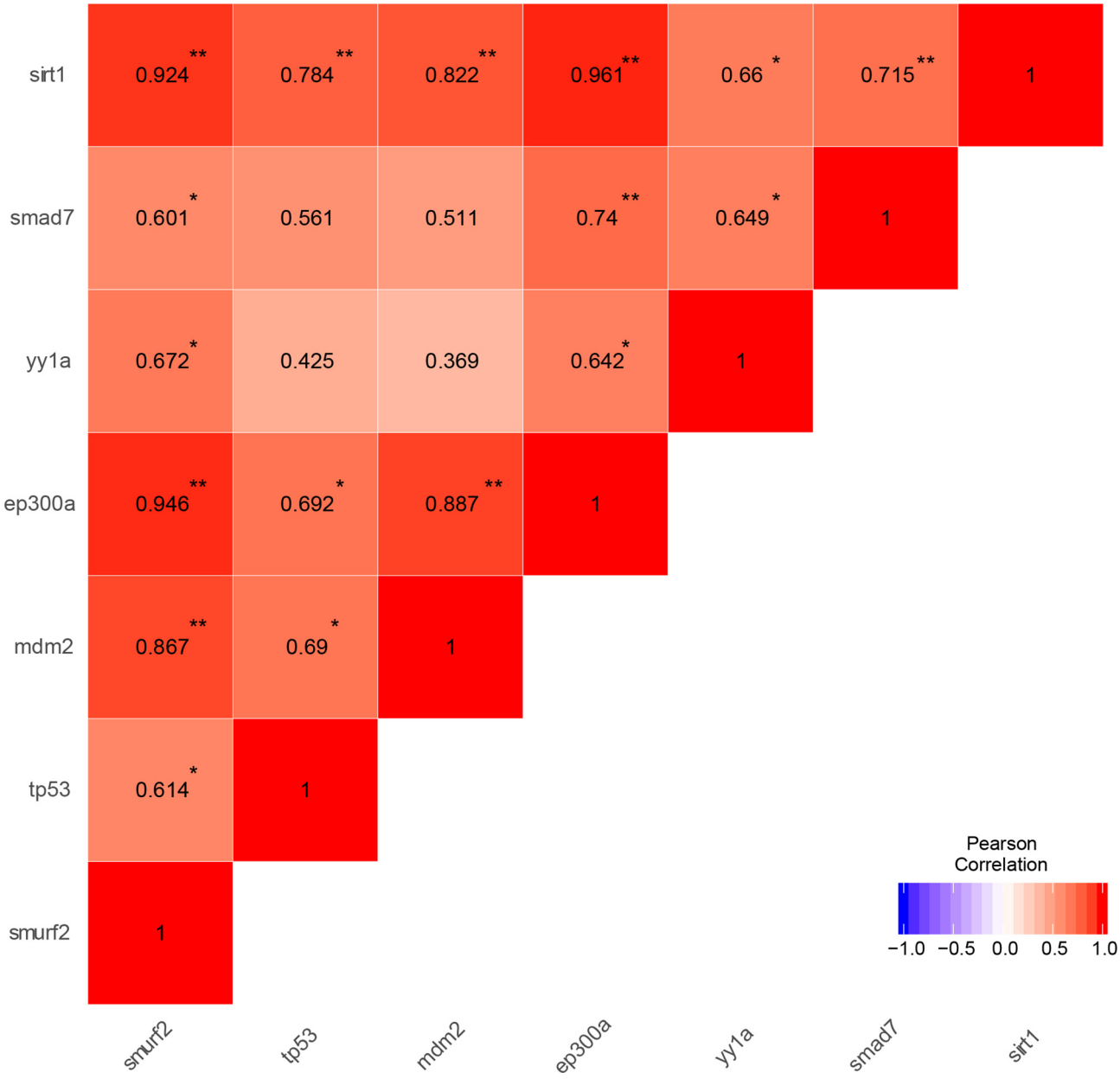

this correlation. Overall, the patterns of correlations between the seven selected genes demonstrated differences between regions (Tables 4–6). To illustrate, in the whole brain data all seven genes were driving the variance together (Table 3) while in the region-specific data certain gene clusters influenced it (Tables 4–6). In the gene expression levels of the whole brain (Fig. 6), we observed that *smurf2*, *ep300a* and *sirt1* impacted the dataset similarly, however, based on the loading plots (Fig. 7) of the region-specific gene expression level analysis, *smurf2* and *sirt1* contributed to the dataset similarly in TeO and Ce, while *ep300a* had comparable influences with *tp53* in TeO (Fig. 7B) and with *smad7* in Ce (Fig. 7C). Furthermore, *smurf2* and *ep300a* had analogous effects on the Tel dataset. As seen in the scatterplots in Fig. 7 the data might indicate that the factor of age had a differential impact on the variance in distinct brain regions. In the light of these results, the data suggest that the expression and interaction of *smurf2*, and its interrelated partners are age- and brain region-specific and they balance ubiquitination, acetylation, and deacetylation in a region-specific manner during aging with each region having its own fingerprint on the balance of these possible PTMs.

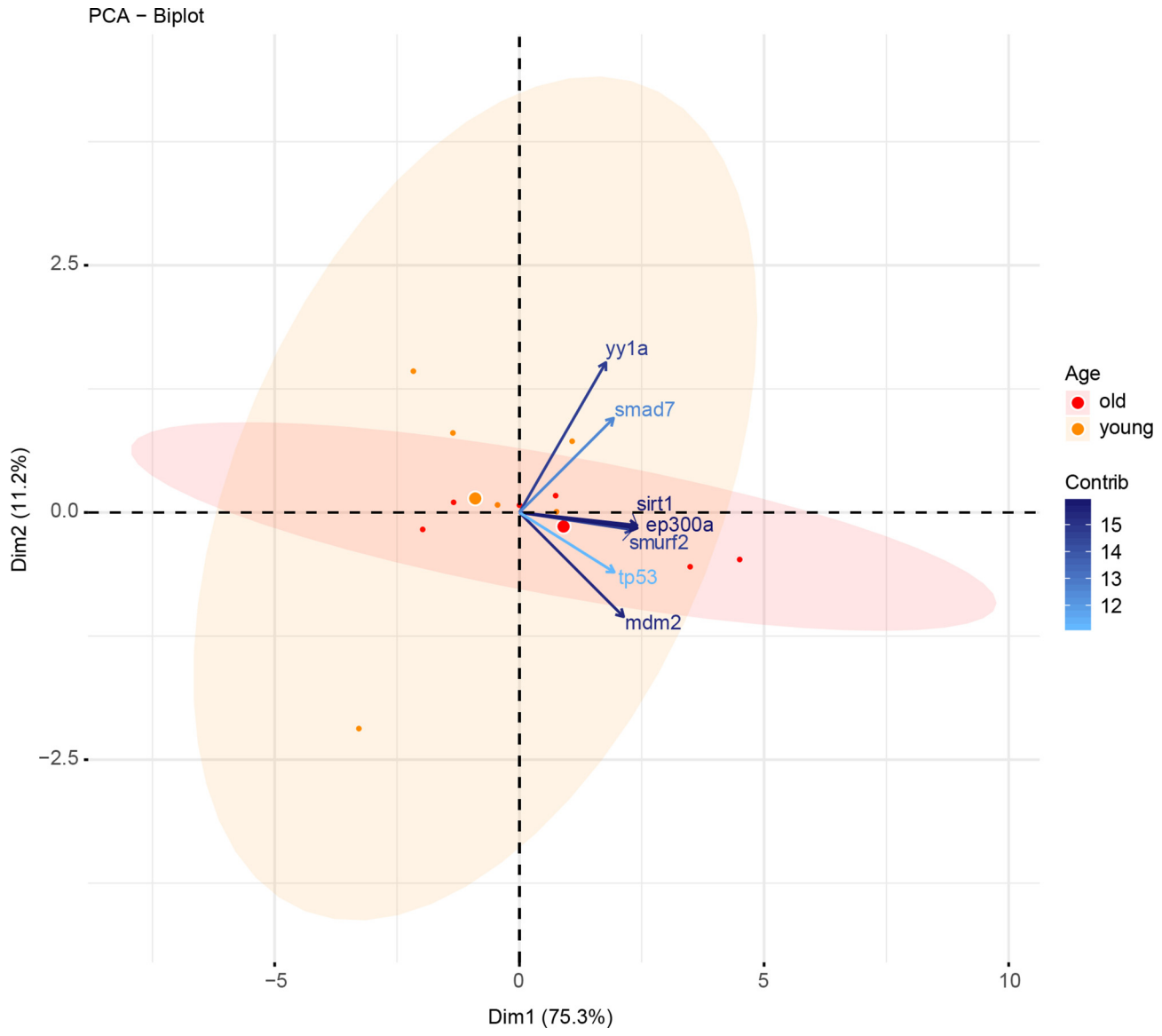

Fig. 6. Loading plot demonstrates gene expression levels of *smurf2* and its interacting partners and a scatterplot of the first and second principal component scores arranged by the factor of age in whole zebrafish brain. Old = red, young = orange. (For interpretation of the references to colour in this figure legend, the reader is referred to the web version of this article.)

DISCUSSION

The current study focused on changes in *SMAD specific E3 ubiquitin protein ligase 2* (*smurf2*) expression levels during brain aging using the zebrafish model organism. Previous data indicate that *smurf2* gene expression levels increase with age in both the brain (Arslan-Ergul and Adams, 2014) and the HSCs (Ramkumar et al., 2014), however, whether or not the protein levels change in a similar manner has not been studied. Thus, in the current study, we aimed firstly to analyze the protein expression levels of Smurf2 in the brain in both a global- and region-specific manner. The results demonstrated that Smurf2 protein levels increased significantly with advanced age in a region-specific manner but not globally in the zebrafish brain. Moreover, Smurf2 protein was enriched in the cytosolic fraction on the zebrafish brain.

In the literature it has been demonstrated that Smurf2 has several interacting partners and also substrates (Fig. 4) because of its role as a ubiquitin E3 ligase. Thus, the next step was to define the interacting partners and analyze their gene expression levels in the aged brain. The gene expression levels of *smurf2* and its interacting partners were analyzed with qRT-PCR to reveal possible age- and region-specific patterns and the data showed that while *smurf2* increased significantly in the old zebrafish brain, *mdm2*, *yy1a*, *sirt1*, and *ep300*a were also rising in the whole brain, whereas *tp53* and *smad7* were stable in the whole brain and the specific 3 brain regions examined. The region-specific gene expression analysis indicated that the expression levels of *smurf2* and its interacting partners were altered region-specifically with aging. Moreover, multivariate statistical testing along with PCA demonstrated that *smurf2*, *ep300a*, and *sirt1* affect

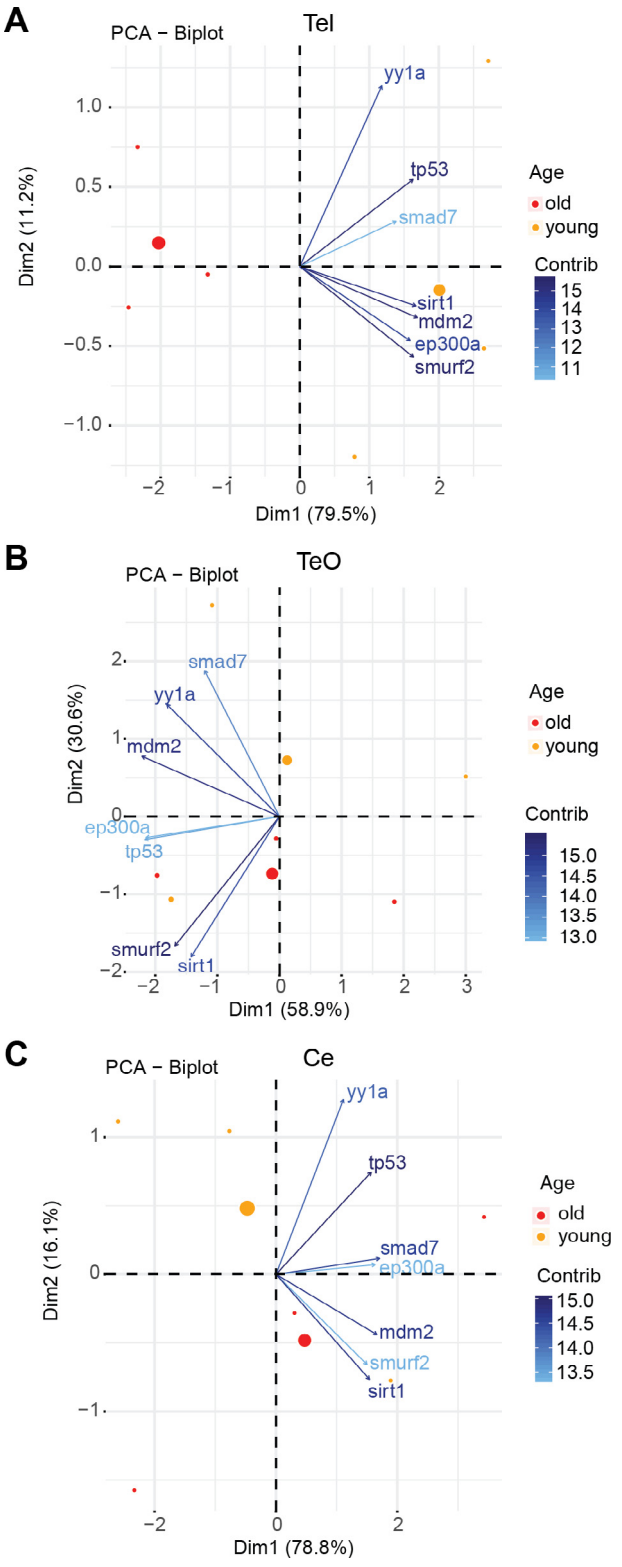

Fig. 7. Loading plots demonstrate gene expression levels of *smurf2* and its interacting partners and the scatterplots of the first and second principal component scores arranged by the factor of age in specific zebrafish brain regions; **(A)** Tel, **(B)** TeO, **(C)** Ce. Old = red, young = orange. (For interpretation of the references to colour in this figure legend, the reader is referred to the web version of this article.)

the dataset in the same way during aging and there are distinct combinations of these three genes based on the brain region, suggesting that there is a balance between ubiquitination, acetylation, and deacetylation during cellular aging in the brain. Moreover, while all seven genes examined in the study correlated with each other in the old group, in young zebrafish, only *smurf2*, *ep300a*, and *sirt1* gene expression levels had a significant relationship with each other (data not shown), suggesting a possible compensatory mechanism to maintain the cellular stability, which is disrupted with age. Thus, this disturbed stability in cellular maintenance is probably due to *smurf2*, *ep300a*, and *sirt1* having multiple regulatory roles in several pathways during aging via ubiquitination, acetylation, and deacetylation, respectively.

Initially, we hypothesized that the increasing pattern of *smurf2* gene expression levels during aging is occurring in parallel with increased protein expression. To test this hypothesis, we used antibodies directed against Smurf2 to determine the protein levels in the aged brain. We also included embryos and larval fish from 2 to 4 dpf in order to validate the antibodies specificity to Smurf2 protein. Our antibodies reacted with the protein motif of the human SMURF2 and it was predicted to work in recognizing the homologous protein in zebrafish tissues. As expected, both antibodies reacted with the cell lysates giving the expected molecular weight of 86 kDa. Although the Smurf2 protein bands of embryos and larvae at 2, 3 and 4 dpf recognized by the anti-SMURF2, 200–300 aa, antibody were at the expected molecular weight of 86 kDa, the anti-SMURF2 C-terminal antibody detected a protein with a slight increase in size (about 100 kDa) in the embryos and larvae. Moreover, in the adult brain a larger molecular weight protein of about 250 kDa was recognized by this antibody, however, the anti-SMURF2, 200–300 aa, and β-tubulin yielded the expected band size in the same tissues. This addresses questions about possible regulatory mechanisms of Smurf2 across lifespan. The information obtained from embryos and adult brain would suggest that there could be a brain-specific PTM on Smurf2 or a potential developmental switch in the regulation of this protein. Thus, increasing *smurf2* gene expression during brain aging influences also protein expression levels of Smurf2, however, this was not detectable with only one antibody because of potential protein modifications. As mentioned in the paper by Li et al. (2002a), acetylation of lysine residues, a PTM, prevented the recognition of tp53 protein by the C-terminal domain-specific antibody, PAb421, because the sites for acetylation of tp53 were overlapping with the PAb421 antibody recognition sites (Li et al., 2002a). Since Smurf2 may also be modified post-translationally, it would be reasonable to speculate that it would react differently with the anti-SMURF2 C-terminal antibody. For example, arginine methylation by protein arginine methyltransferase 1 (PRMT1) regulates Smurf2 expression (Cha et al., 2015). It has been shown that PRMT1 methylates arginine residues at the 234 and 239 amino acid positions of the human SMURF2, and the knockdown of PRMT1

Table 4. Correlation matrix of target genes of interest in zebrafish Tel. Significance of correlation coefficients (2-tailed): *$p < 0.05$, **$p < 0.01$. ($n = 6$ per region)

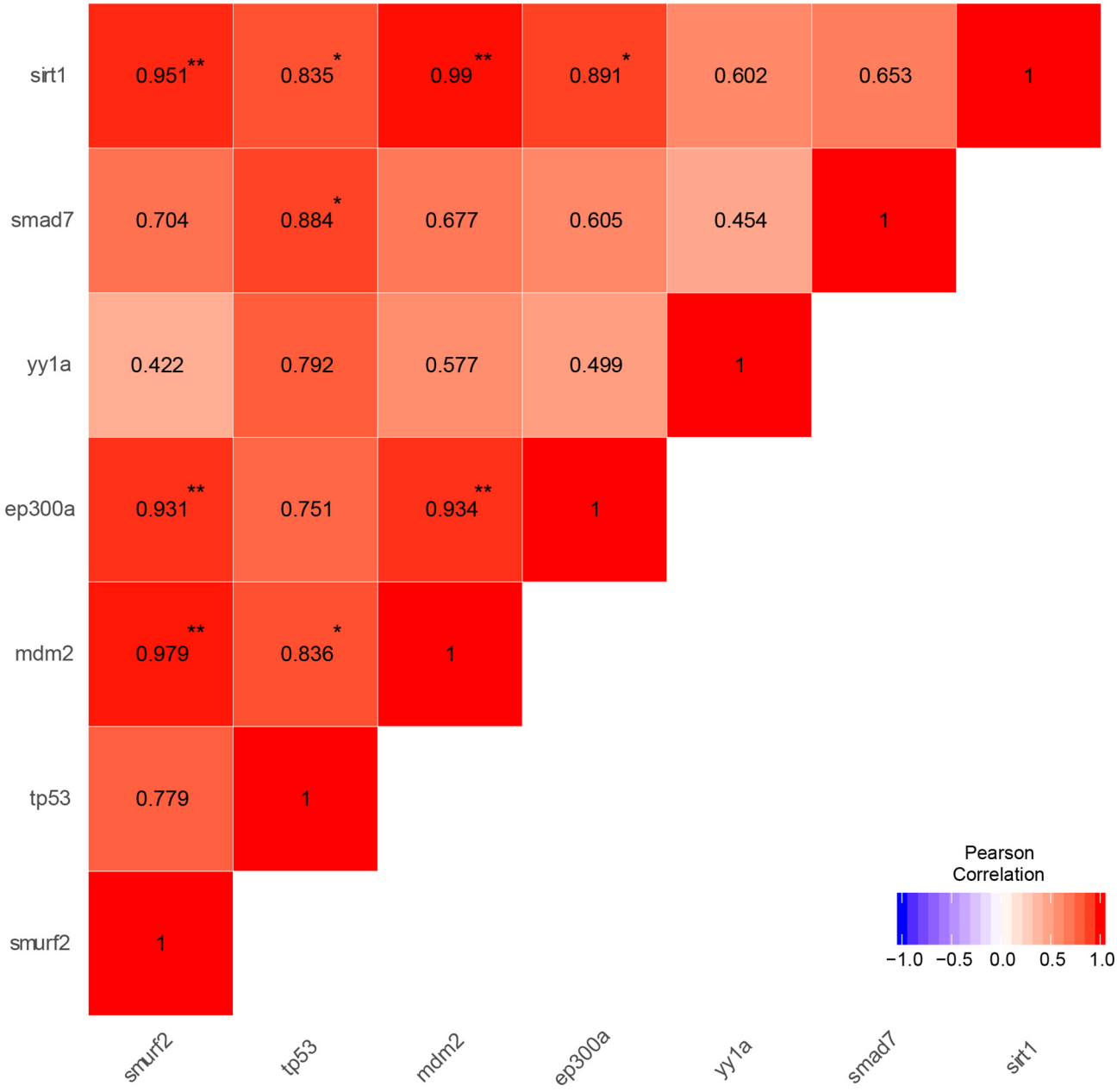

causes an upregulation of the level of Smurf2 (Cha et al., 2015). It is possible that the anti-SMURF2, 200–300 aa, recognizes unmethylated Smurf2 because the methylated arginine residues overlap with the anti-SMURF2, 200–300 aa, antibody recognition sites, and thus methylation prevents the binding between the Smurf2 antigen and the anti-SMURF2, 200–300 aa, antibody. However, the anti-SMURF2 C-terminal recognizes the methylated version of Smurf2 due to its recognition site being independent of those for methylation. Also, it has been demonstrated that Smurf2 level and activity is under control of other PTMs such as sumoylation and autoubiquitination (Wiesner et al., 2007; Chandhoke et al., 2016). However, one of these PTMs would likely not increase the molecular weight size as observed in the current study. One other possibility is the complex formation of the Smurf2 protein with interacting partners such as a Smurf2-Smad7 complex (Wiesner et al., 2007). The activated Smurf2-Smad7 complex causes TGF-β receptor complex degradation in the cytosol (Kavsak et al., 2000) or targets nuclear substrates for ubiquitin-mediated degradation (Wiesner et al., 2007). It is also possible that

Table 5. Correlation matrix of target genes of interest in zebrafish TeO. Significance of correlation coefficients (2-tailed): *$p < 0.05$, **$p < 0.01$. ($n = 6$ per region)

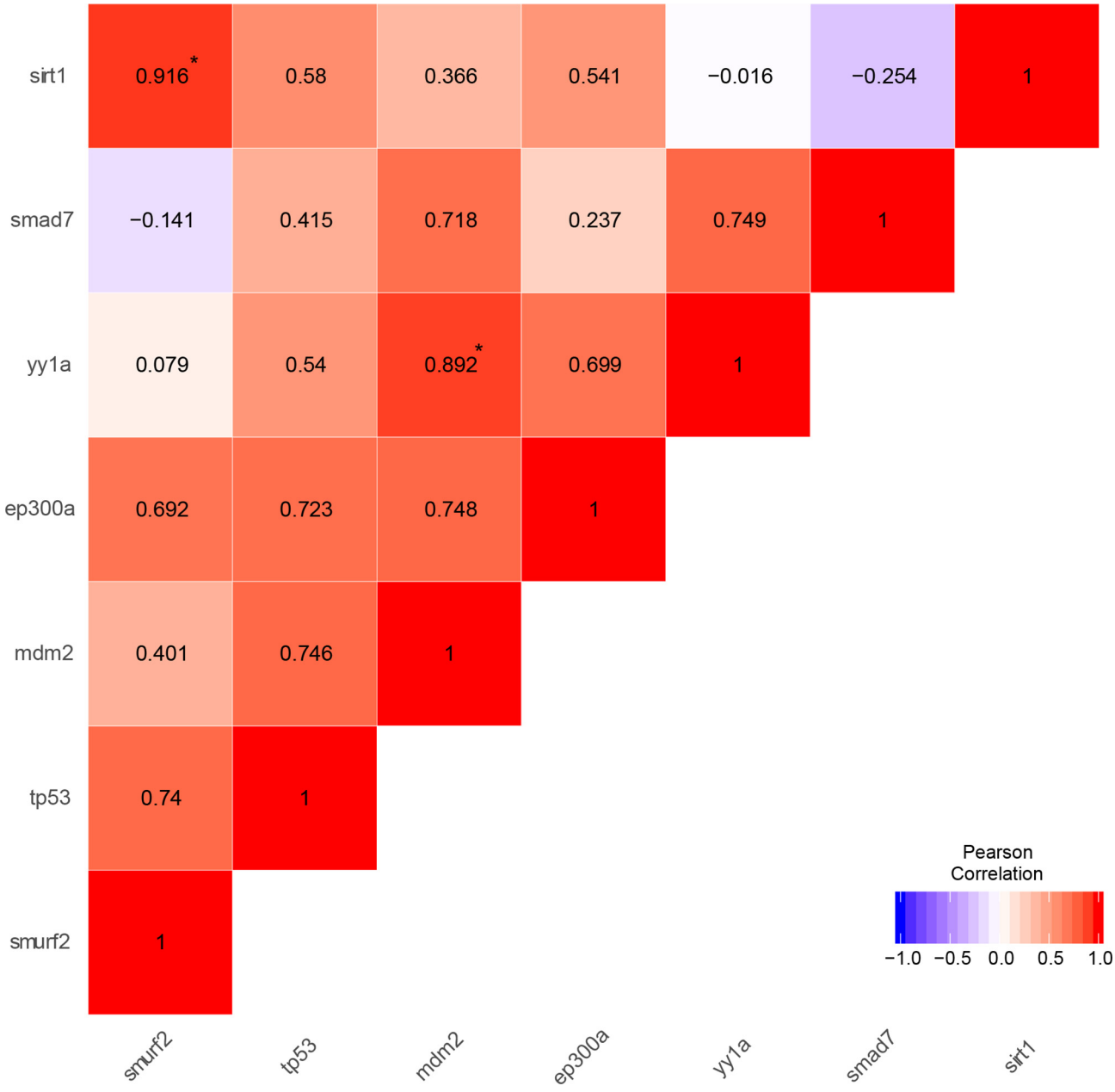

similar to the study by Emanuelli et al., (2019), the anti-SMURF2, 200–300 aa antibody binds to cytosolic Smuf2 but not in a complex (86 kDa) and independent of PTMs, whereas anti-SMURF2 C-terminal antibody recognizes the Smurf2 complex structure. While we strongly believe that the changes in molecular weight represent either a Smurf2 protein complex or multiple PTMs of different origins, of course we cannot eliminate the possibility that the antibody, anti-Smurf2, 200–300 aa, cannot bind to the complexed Smurf2 because the recognition site is not available. Further analysis with immunoprecipitation or mass spectrometry of the protein structure of Smurf2 and its complex structures, as well as its PTMs, should be performed in order to delineate whether or not there are differences in the complex structure formation or PTMs across lifespan.

In embryos and larvae at 2, 3 and 4 dpf, we observed a slightly larger band than the expected 86 kDa and smaller band than in the adult brain. Since all the main parts of the central nervous system, including the brain, have formed by 5 dpf (Nüsslein-Volhard and Dahm, 2002), any changes in the state of the Smurf2 protein are most likely reflected in these areas. As development continues past this point, Smurf2 would also be involved in the maturation of these areas. It has been shown that in early Xenopus embryogenesis Smurf2

Table 6. Correlation matrix of target genes of interest in zebrafish Ce. Significance of correlation coefficients (2-tailed): *$p < 0.05$, **$p < 0.01$. ($n = 6$ per region)

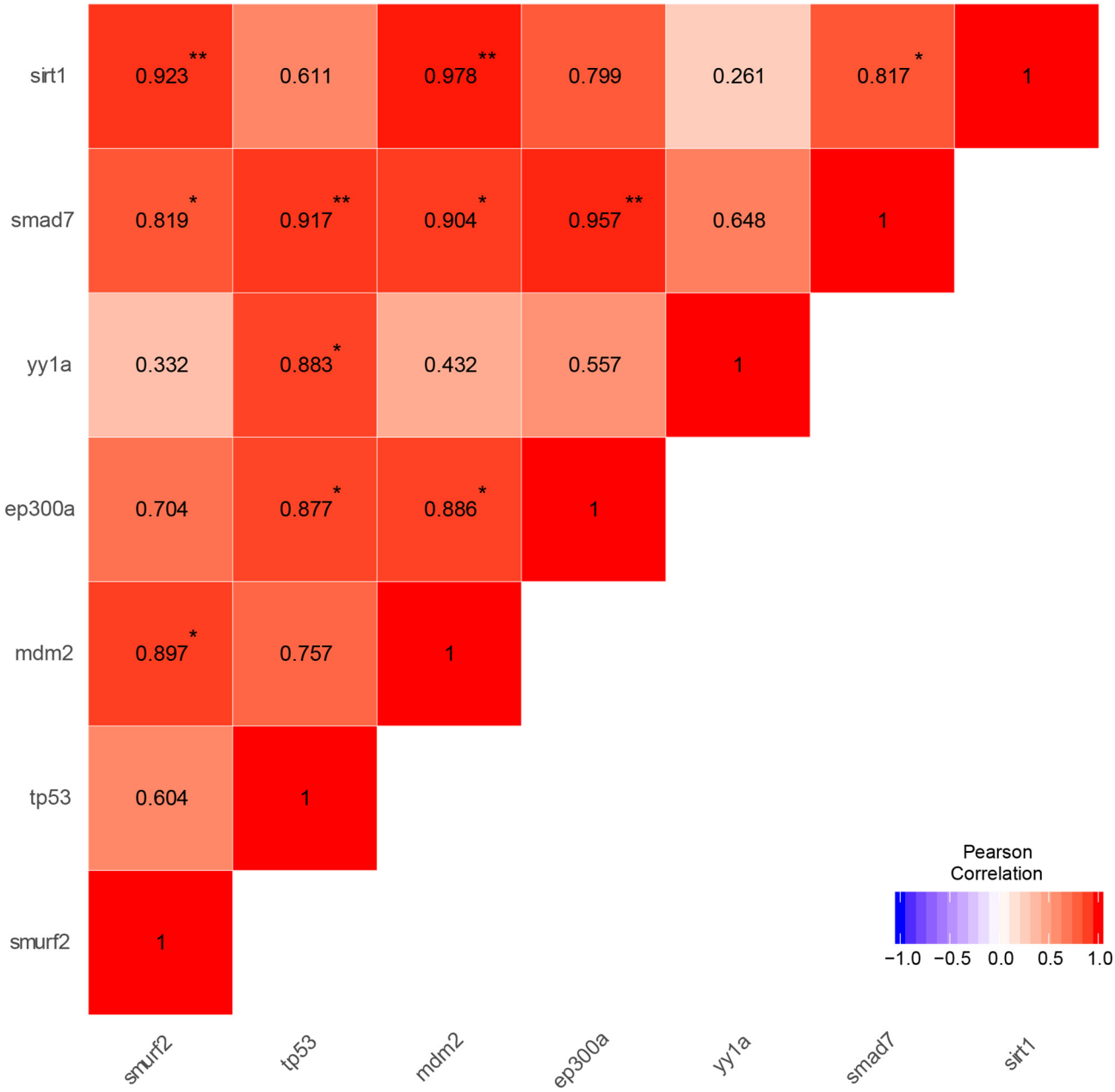

modulates neural development and regulates several markers at the neural plate border (Das and Chang, 2012). Additionally, it is known that the TGF-β signaling pathway is needed during embryogenesis and for proper development (Tominaga and Suzuki, 2019). Moreover, the signaling transmission depends on the ligand, tissue, and developmental stage, which indicates that TGF-β signaling is context-dependent and likely increased during early development (Hata and Chen, 2016). Research has demonstrated that the Smurf2-Smad7 complex in the cytosol will degrade the TGF-β receptor complex and this ultimately results in less signaling (Kavsak et al., 2000). In the current study, the Smurf2 band detected at 100 kDa in embryos should indicate a protein with many PTMs not a complex formation of Smurf2 with Smad7 because that would be much larger than 100 kDa. Additionally, during this period the TGF-β receptor protein levels should be stabilized and not degraded by a Smurf2-Smad7 complex in order to maintain the TGF-β signaling for proper development. Further developmental time points should be examined for the functional regulation of Smurf2.

To test our initial hypothesis as to whether Smurf2 protein levels increase during brain aging in parallel with *smurf2* gene expression levels, two different anti-SMURF2 antibodies were used to examine the effects of age and brain region. Whereas the protein levels in the whole brains of old zebrafish did not increase significantly as compared to young animals, the analysis of the microdissected brain regions including the telencephalon (Tel), optic tectum (TeO) and the cerebellum/medulla/spinal cord (Ce), demonstrated an upregulation in the Tel with two different antibodies. Moreover, protein expression determined by anti-SMURF2 C-terminal antibody showed also a significant increase in Ce. Since the Tel represents about 18% of brain volume and Ce represents about 33% of total brain volume (Ullmann et al., 2010), it is reasonable to observe a numerical increase in whole brain Smurf2 protein level as determined by the anti-SMURF2 C-terminal antibody. Importantly, both antibodies demonstrated that Smurf2 protein levels increased with age but it was region-dependent and only in one region, Ce, did we see differences between the two antibodies. The fact that there were age-related increases in the Tel region that occurred across both antibodies reflects the point that these changes in Smurf2 are robust in that area. Smurf2 is a ubiquitin E3 ligase regulating several important pathways (David et al., 2013) and has roles in senescence (Zhang and Cohen, 2004). Interestingly, we reported that SA-β-gal levels in Tel also increase with advanced age (Arslan-Ergul et al., 2016) and thus, Smurf2 protein accumulation in this region might be protective by maintaining proteostasis and an underlying reason for senescence to occur or the consequence of senescence. Neurogenesis in this area decreases with advancing age in Tel (Edelmann et al., 2013; Arslan-Ergul et al., 2016). Previous research indicated that different parts of Tel have roles in the sensory, motor and cognitive functions including learning and memory (Ganz et al., 2014). Moreover, the putative homologues of mammalian hippocampus and amygdala were defined in the zebrafish Tel region (Ganz et al., 2014). Recent studies has shown LTP of synaptic plasticity occurs in the Tel region of zebrafish brain (Nam et al., 2004; Ng et al., 2012; Wu et al., 2017). Since the Tel is a more prominent region with respect to cognitive functions including learning and memory in zebrafish, age-responsive Smurf2 alterations as reported in the current study imply a role for Smurf2 during aging and age-related cognitive alterations. Currently there are no antibodies that recognize the Smurf2 protein that work for performing immunohistochemical analysis in the zebrafish brain. As antibodies develop, further anatomical studies should be performed.

As mentioned previously, Smurf2 has several substrates and interacting partners, which are also involved in diverse regulatory roles in cellular processes. In the current study, we confirmed that the gene expression levels of *smurf2* increase significantly in the aged brain, as was shown previously in both brain tissues and HSCs (Arslan-Ergul and Adams, 2014; Ramkumar et al., 2014). However, when we investigated gene expression levels in the three main regions of the zebrafish brain, we found that *smurf2* levels decreased in Tel and Ce during aging. Despite there being a down-regulation of *smurf2* in the Tel and Ce regions, upregulated protein levels were observed in the same regions and support the hypothesis that Smurf2 accumulated in the aged brain and possibly maintains proteostasis in more vulnerable regions of the brain to aging. Moreover, while the gene expression levels of smurf2 in the whole brain increased, there was a significant decrease in the Tel and Ce regions, which sums up approximately 50% of zebrafish brain volume. The three microdissected pieces from each of the three animals in the same age group were pooled together to obtain enough concentrations of mRNA for subsequent analysis. However, as a drawback of the microdissection of a small brain, there is a large possibility of losing some small portions of the brain during this procedure. This may account for some of the discrepancies between the whole brain and region-specific analyses.

The aim of STRING analysis was to display the interacting partners of Smurf2 in zebrafish. After defining the interacting partners computationally, which have also known roles in aging and senescence, their gene expression patterns levels were analyzed to determine whether or not there were significant correlations between them in the aged zebrafish brain. In contrast to *smurf2* expression levels, surprisingly, the other interacting partners did not change significantly although there were numerical increases in some with *tp53* and *smad7* remaining absolutely stable during brain aging. The expression levels of *mdm2* increased marginally in the aged brain of zebrafish and decreased in a region-specific manner in the Tel. MDM2 regulates tp53 during normal aging and the balance between tp53 and MDM2 prevents the cells from tp53-mediated senescence, which results in an early aging phenotypes (Lessel et al., 2017; Wu and Prives, 2018). Like MDM2, YY1 is also a negative regulator of tp53 (Sui et al., 2004). The expression levels of *yy1a* and *sirt1* were slightly elevated in the aged zebrafish brain in our gene expression analysis. YY1, a transcription factor, regulating genes associated with neurodegenerative diseases (Li et al., 2014). Also, it has been shown that YY1 is part of a repressor complex with SIRT1 to suppress microRNA-134 (miR-134) and the upregulation of YY1. In addition, the upregulation of SIRT1 activates cAMP response binding protein (CREB) expression, which enhances synaptic plasticity and memory formation (Gao et al., 2010). Recent studies indicate that the protein expression of SIRT1 decreases during aging in the hypothalamus (Sasaki, 2015), heart (Gu et al., 2013) and vascular tissue undergoing senescence (Kitada et al., 2016). Moreover, SIRT1 protects against neurodegeneration in models of Alzheimer's disease and amyotrophic lateral sclerosis by promoting neuronal survival via tp53 deacetylation (Kim et al., 2007). Deacetylation destabilizes tp53 and may promote its degradation by the ubiquitin–proteasome system (Li et al., 2002a; Solomon et al., 2006; Kim et al., 2007). Previous studies in mice and rats demonstrated that while the protein expression of Sirt1 reduces with age, the gene expression level changes of *sirt1* during aging are gender-dependent

and specific to particular brain areas such as the hypothalamus, hippocampus, and cortex; old mice has lower *sirt1* mRNA levels in the hypothalamus (Lafontaine-Lacasse et al., 2010; Quintas et al., 2012). Our current study used whole brain tissues of zebrafish from young and old animals and included both males and female subjects, and the increase of *sirt1* in the old brain was driven by female samples (data not shown). This would suggest that *sirt1* gene expression during aging may be sexually dimorphic and might vary differentially in specific brain regions in zebrafish as well. In the current study, brain region-specific analysis of *sirt1* expression showed that it was altered depending on which region was examined in the aged brain.

In the current study, *ep300a* expression increased numerically but was not statistically significant in the whole brain but it decreased in the Tel region of the aged zebrafish. Previously, Li et al. (2002b) indicated that the gene expression level of *ep300* in mice liver decreased with age while the *ep300* expression levels in other tissues were stable in old mice. Similarly, distinct brain regions showed different patterns in the aged brain according to our region-specific analysis. Recently, it was shown that ep300 protein expression levels increase in aged mice livers (Nguyen et al., 2018), while in senescent cells ep300 protein levels were decreasing (Sen et al., 2019). Taken together with the current results, *ep300a* expression levels may change according to the type of tissues or even the specific brain region, as well as the state of proliferation or senescence. On the other hand, we demonstrated that *tp53* and *smad7* expression was stable during brain aging in zebrafish. Since tp53 has a short half-life and its activity is tightly regulated by several processes including PTMs such as ubiquitination, phosphorylation, and acetylation (Hasegawa and Yoshikawa, 2008; Ou and Schumacher, 2018), its expression may be under tight regulatory control and kept stable during aging. However, it was shown that tp53 protein levels increased in cells such as astrocytes derived from aged individuals (Bitto et al., 2010). Furthermore, in the neurogenic brain regions such as the hippocampus, subventricular zone (SVZ), and olfactory bulb, *Smad7* mRNA levels are higher than the levels in non-neurogenic brain regions including cortex and striatum, since Smad7 regulates neural stem/progenitor cell proliferation in the mice brain (Krampert et al., 2010). In the current study, *smad7* mRNA levels remained at a comparable level during aging in the zebrafish brain. Although previous studies showed region-specific alterations in *Smad7* levels (Krampert et al., 2010; Marschallinger et al., 2014), the current study did not indicate any significant changes due to age and region. As we know, zebrafish produce new neurons along the rostrocaudal brain axis throughout their lifespan, which is contrary to the mammals (Kizil et al., 2012) and 16 distinct proliferative zones have been described in the zebrafish brain (Grandel et al., 2006). These neurogenic zones are distributed along the entire brain, and thus this would be consistent with the fact that we did not observe any distinct region-dependent alterations in *smad7* expression levels with advanced age.

PCA demonstrated that *smurf2*, *ep300a*, and *sirt1* expression levels had similar contributions to the variance of the data and they were significantly correlated with each other. The comparable trend of these genes; *smurf2*, *ep300a*, and *sirt1*, would imply that their proteins are regulating common targets via different PTMs such as ubiquitination, acetylation, and deacetylation, respectively. For example, it has been well documented that Smurf2 influences MDM2, tp53, YY1, and Smad7 levels via ubiquitination (Kavsak et al., 2000; Nie et al., 2010; Jeong et al., 2014) while ep300, a transcriptional co-activator, acetylates tp53, YY1, and Smad7 (Ito et al., 2001; Grönroos et al., 2002, 2004), and conversely, SIRT1 deacetylates Smad7 (Kume et al., 2007) and tp53 (Vaziri et al., 2001; Solomon et al., 2006). Moreover, it is known that acetylation and ubiquitination compete to control the stability of Smad7 (Grönroos et al., 2002; Simonsson et al., 2005), while it functions cooperatively with YY1 and additional proteins underlying synaptic plasticity (Gao et al., 2010). Acetylation of Smad7 by ep300 protects it from ubiquitin-mediated degradation (Grönroos et al., 2002). However, YY1 inhibits ep300-mediated tp53 acetylation and tp53-activated transcription (Grönroos et al., 2004), and additionally, YY1 physically interacts with Mdm2, which is also a negative regulator of tp53 (Sui et al., 2004; Inoue et al., 2016). MDM2 also regulates tp53 stability with the help of other factors such as Smurf2 and ep300 as well as YY1 (Ito et al., 2001; Nie et al., 2010), and these four regulate different post-translational mechanisms, although they have the same target proteins. In brief, Smurf2 ubiquitinates Smad7, while ep300 acetylates it and SIRT1 deacetylates it. Also, Smurf2 affects the ubiquitination state of tp53 and ep300 acetylates tp53, while SIRT1 deacetylates it. Since they share the target proteins and one modification will affect the others (Yao et al., 2001; Simonsson et al., 2005; Solomon et al., 2006), it is likely that they have similar contributions to cellular aging in the brain.

Our multivariate analysis completed with PCA also indicated that *yy1a* had a different influence on the covariance and there was no correlation between *yy1a* and *mdm2* in the whole brain. As well as *yy1a* and *mdm2*, *yy1a* was not correlated with *smurf2* and *sirt1* in the brain region-specific gene expression analysis except TeO. Interestingly, gene expression levels of TeO indicated a correlation between *yy1a* and *mdm2*. Since both MDM2 and YY1 are negative regulators of tp53 (Sui et al., 2004; Nie et al., 2010) and they can interact physically with each other (Sui et al., 2004; Inoue et al., 2016), it is likely that they compete or compensate during aging. Our PCA analysis indicated that their contribution to the variance was in the opposite direction and may support the idea of competition or compensation. Additionally, while YY1 suppresses tp53 (Sui et al., 2004), it inhibits tp53 acetylation by ep300 (Grönroos et al., 2004), and Smurf2 relieves the suppression of YY1 on tp53 activity (Jeong et al., 2014). Since MDM2 also regulates tp53 stability in similar ways with the help of other factors such as Smurf2 and ep300 (Ito et al., 2001; Nie et al., 2010), it may compete with YY1 or

compensate YY1 activity in the regulation of tp53 while it may work coordinately with YY1 in TeO to overcome region-specific needs. However, the similar contribution of *smurf2*, *ep300a*, *and sirt1* to the variance in the qRT-PCR dataset would demonstrate that these genes in the zebrafish brain likely influence the other target genes of interest. Previous studies indicated that both acetylation and ubiquitination modify the same lysine residues of tp53 and there is a balance between acetylation/deacetylation and ubiquitination on the stability of Smad7 (Li et al., 2002a; Brooks and Gu, 2003; Simonsson et al., 2005). Furthermore, SIRT1 has a role in neuronal survival via tp53 deacetylation (Kim et al., 2007; Hasegawa and Yoshikawa, 2008). Thus, there may be a balance between ep300a-mediated acetylation/Sirt1-mediated deacetylation and Smurf2-mediated ubiquitination during brain aging. Since Smurf2 and its interacting partners regulate each other and they were regulated by several PTMs, it will be necessary to determine the protein expression levels of interacting partners during brain aging as well as their functional protein–protein interactions. Moreover, further steps should be done that to unravel the causative interactions between their proteins.

Although there have been many studies about the role of Smurf2, they were generally analyzed in the context of cancer progression. In the review by David et al., (2013), Smurf2 was described as a double-edged sword because of its function in both tumor suppression and promotion. This implied that Smurf2 has roles in several cellular pathways including senescence (Zhang and Cohen, 2004; Kong et al., 2011), telomere attrition (Zhang and Cohen, 2004), stem cell self-renewal (Ramkumar et al., 2014), and genomic stability (Blank et al., 2012) as well as ubiquitin-mediated proteasomal degradation (David et al., 2013). Genomic instability, telomere attrition, loss of proteostasis, cellular senescence and stem cell exhaustion are also occurring during aging and are described as some of the hallmarks of aging (López-Otín et al., 2013). Both the gene and the protein expression levels of *smurf2* increased with advancing age in the brain. Our previous studies also demonstrated that during aging, the number of senescent cells increases in the brain (Arslan-Ergul et al., 2016). Cellular senescence is defined as an antagonistic hallmark of aging (López-Otín et al., 2013) because it is a response to damaged or aged cells (Muñoz-Espín and Serrano, 2014). Moreover, senescence is thought to be a central hallmark of aging (McHugh and Gil, 2018) because telomere attrition and genomic instability trigger the senescence response and the others have several links with senescence. As a response to telomere shortening in fibroblasts, Smurf2 was upregulated and this increase was sufficient to trigger a senescent phenotype (Zhang and Cohen, 2004). It has been shown that Smurf2 regulates senescence via the p16 (Kong et al., 2011) or the p53-p21 pathways (Zhang and Cohen, 2004; Nie et al., 2010). The ubiquitination and consequent degradation of the inhibitor of differentiation or DNA binding 1 (Id1) by Smurf2 provide a link between Smurf2 and p16 during senescence (Kong et al., 2011). The study by Ramkumar et al., (2012) demonstrated that in the spleen of Smurf2-deficient mice there was decreased SA-β-gal activity, a senescence marker, and lower p16 gene and protein expression levels, which is another indicator of senescence (Krishnamurthy et al., 2004). This suggests that the absence of Smurf2 leads to a delayed senescence response. Moreover, an age-dependent increase of p16 expression is associated with a decline in stem cell self-renewal in brain, pancreas, and hematopoietic system (Kong et al., 2011; Ramkumar et al., 2014). Consistent with this, senescence inducers such as telomere attrition and oxidative stress cause DNA damage and this activates a kinase cascade to trigger tp53 activation (McHugh and Gil, 2018). Furthermore, sirtuins establish a link between metabolism and senescence, for instance, SIRT1 deacetylates tp53 and promotes its degradation with ubiquitin-mediated proteolysis (Solomon et al., 2006), and prevents senescence (McHugh and Gil, 2018). On the other hand, Smurf2 has a role in genomic stability through the ring finger protein 20 (RNF20), which also regulates genomic stability and the chromatin landscape (Blank et al., 2012). The other regulatory role of Smurf2 is in stem cell exhaustion, which is an integrative hallmark of aging (López-Otín et al., 2013). It has been shown that the function of HSCs declines with age in a Smurf2-dependent manner such that Smurf2-deficient mice have an absence of the premature exhaustion of HSCs, and thus, Smurf2-deficient HSCs had increased self-renewal capacity (Ramkumar et al., 2014). In the review of Wu and Prives (2018), the authors indicated that the p53 pathway is a master regulator of three hallmarks of aging; genomic stability, mitochondrial dysfunction, and cellular senescence. Moreover, several findings suggested that the cooperation of tp53 and SIRT1 is required for genomic stability (Yi and Luo, 2010), and alternatively, the downregulation of ep300, which acetylates tp53, YY1, and Smad7, delays senescence (Sen et al., 2019).

It has been demonstrated that there is no significant cellular (Rapp and Gallagher, 1996; Rapp et al., 2002) or synaptic loss (Calhoun et al., 1998; Poe et al., 2001; Shi et al., 2007; Newton et al., 2008) in the aged brain. It is likely subtle cellular and synaptic alterations that are contributing to this aging process (Ganeshina et al., 2004; Adams et al., 2008; VanGuilder et al., 2010, 2011). In this study, we focused on the molecular changes which are possibly affecting the cellular and synaptic changes during aging, as well. It has been shown that SIRT1 is expressed in the neurons of hippocampus and has a role in synaptic plasticity and so learning and memory (Gao et al., 2010; Michan et al., 2010). A repressor complex including SIRT1 and YY1 suppresses brain-specific miR-134 which regulates the expression of CREB and brain-derived neurotrophic factor (BDNF) (Gao et al., 2010). Since these proteins are important for synapse formation and LTP, the suppression on miR-134 is relieved in SIRT1 knockout mice and it causes the decreased LTP in the CA1 region of the hippocampus and thus impaired memory (Gao et al., 2010; Michan et al., 2010). Moreover, SIRT1 has protective roles in neurodegenerative diseases including Alzheimer's and Parkinson's diseases. For example, SIRT1 deacetylates Tau and promotes the clearance of Tau by proteasome-

mediated degradation (Min et al., 2010; Herskovits and Guarente, 2014) while ep300 acetylates Tau (Min et al., 2010). The inhibition of ep300 promotes Tau deacetylation and eliminates phosphorylated Tau associated with neurodegenerative diseases such as in Alzheimer's disease (Min et al., 2010). Additionally, in the context of the regulation of Tau, SIRT1-mediated deacetylation and ep300-mediated acetylation and even phosphorylation and ubiquitination work to create an important balance to maintain the normal cellular processes that will promote intact cognitive function. In addition, it has been shown that the overexpression of 'EP300 interacting inhibitor of differentiation 1' (EID1) protein, which is highly expressed in neurons of mouse and human brains, leads to decreases in LTP and impairs spatial learning and memory because the increased inhibitory function on acetyltransferase activity of ep300 affects the expression and post-translational regulation of target proteins such as the acetylation of tp53 (Liu et al., 2012). Tedeschi and Di Giovanni, (2009) indicated that during neuronal outgrowth and maturation, the ep300-mediated acetylation of tp53 increased in neuronal cells. Recent studies showed that loss of fragile X mental retardation protein (FMRP) affects tp53, MDM2, and EP300 in neurons and subsequently synaptic downscaling and hyperexcitability (Lee et al., 2018) and adult neurogenesis and cognition (Li et al., 2018). The loss of FMRP stabilizes tp53 in neurons which decreases the ubiquitination of the GluA1 subunit of the AMPA receptor and synaptic downscaling with the help of other interacting partners such as MDM2 and Nedd4-2 (Lee et al., 2018). Moreover, as a result of FMRP downregulation, both the protein levels of EP300 and MDM2-mediated ubiquitination and degradation of the histone deacetylase, HDAC1, increases in adult hippocampal neural stem cells (NSCs). Thus, unbalanced histone acetylation in FMRP-deficient NSCs results in cognitive impairment whereas reducing histone acetylation restores neurogenesis and cognition in adult FMRP-deficient mice (Li et al., 2018). Taken together with all information, the combination of subtle changes in the molecular level has an influence on the synaptic and cognitive levels.

The aforementioned Smurf2 and its interacting genes and their roles in the hallmarks of aging specifically in senescence imply that *smurf2* and other master regulators such as *tp53* and *ep300a* have roles in brain aging and future studies should examine their functional roles in more detail. Moreover, inducible overexpression models of Smurf2 may help to clarify its role in senescence and aging regulation of its interacting partners. Due to the elaborate network between Smurf2 and the aforementioned interacting proteins, a Smurf2 overexpression model may be used to study premature aging and even neurodegenerative diseases via its interacting partners such as Sirt1, tp53, and ep300.

In summary, Smurf2 has several roles in various cellular processes and most of them are related to a few key hallmarks of aging like genomic instability, telomere attrition, and cellular senescence. Thus, we studied the levels of *smurf2* gene and protein expression during brain aging. Our previous data indicated that gene expression levels of *smurf2* increased with age (Arslan-Ergul and Adams, 2014), so we hypothesized that Smurf2 protein expression would also increase with age and its interacting partners would be affected by this upregulation. Our study demonstrated that Smurf2 protein levels increase in a brain region-specific manner with age. Moreover, the gene expression levels of the critical interacting partners and substrates of Smurf2 were analyzed and our findings indicate that *smurf2* and its interacting partners, *ep300a* and *sirt1*, have a similar contribution to the variance of data and are highly correlated. Thus, it is likely that Smurf2, Mdm2, ep300a and Sirt1 affect the stability of Smad7, yy1a, and tp53. To our knowledge, this study is one of first that focuses on Smurf2 and its several interacting partners during brain aging and our data indicate that the changes in Smurf2 might underlie subtle cellular changes, especially in senescence and proliferation that contribute to cognitive decline.

ACKNOWLEDGEMENTS

The authors would like to thank Tulay Arayici for excellent technical assistance with the experiments in the zebrafish facility, Ergul Dilan Celebi-Birand for helpful discussion and Resat Sasik for helping with preparation of the figures.

AUTHOR CONTRIBUTION

MUT-S designed and performed the experiments, as well as contributed to writing of the manuscript. AA-E and MK contributed to the initial planning of the experiments. ETK-E and MK performed statistical analysis. MMA conceived of the study, participated in its design, helped to write and finalize the manuscript. All authors read and approved the final version of the manuscript.

FUNDING

This work was supported by a EMBO Installation Grant (Funds provided by TUBITAK) to Michelle M. Adams. The authors, MUT-S and ETK-E, were supported by the TUBITAK 2211- National Graduate Scholarship Programme (BIDEB). The author MK was supported by the TUBITAK 2209A- University Students Domestic Research Projects Support Program.

DECLARATION OF COMPETING INTEREST.

The authors declare that they have no competing interests.

REFERENCES

Adams MM, Shi L, Linville MC, Forbes ME, Long AB, Bennett C, Newton IG, Carter CS, Sonntag WE, Riddle DR, Brunso-Bechtold JK (2008) Caloric restriction and age affect synaptic proteins in hippocampal CA3 and spatial learning ability Available at:. Exp Neurol 211:141–149.

Ain Q, Schmeer C, Penndorf D, Fischer M, Bondeva T, Förster M, Haenold R, Witte OW, Kretz A (2018) Cell cycle-dependent and -independent telomere shortening accompanies murine brain aging Available at:. Aging (Albany NY) 10:3397–3420.

Arslan-Ergul A, Adams MM (2014) Gene expression changes in aging Zebrafish (Danio rerio) brains are sexually dimorphic Available at:. BMC Neurosci 15:29.

Arslan-Ergul A, Erbaba B, Karoglu ET, Halim DO, Adams MM (2016) Short-term dietary restriction in old zebrafish changes cell senescence mechanisms. Neuroscience 334:64–75. https://doi.org/10.1016/j.neuroscience:2016.07.033.

AVMA (American Veterinary Medical Association) (2013) AVMA guidelines for the Euthanasia of Animals: 2013 Edition. Available at: available: https://www.avma.org/kb/policies/documents/euthanasia.pdf. (January 2018).

Babu A, Kamaraj M, Basu M, Mukherjee D, Kapoor S, Ranjan S, Swamy MM, Kaypee S, Scaria V, Kundu TK, Sachidanandan C (2018) Chemical and genetic rescue of an ep300 knockdown model for Rubinstein Taybi Syndrome in zebrafish. Bioch Biophys Acta 1864:1203–1215. https://doi.org/10.1016/j.bbadis.2018.01.029.

Becker T, Wullimann MF, Becker CG, Bernhardt RR, Schachner M (1997) Axonal regrowth after spinal cord transection in adult zebrafish Available at:. J Comp Neurol 377:577–595.

Bitto A, Sell C, Crowe E, Lorenzini A, Malaguti M, Hrelia S, Torres C (2010) Stress-induced senescence in human and rodent astrocytes. Exp Cell Res 316(17):2961–2968. https://doi.org/10.1016/j.yexcr.2010.06.021.

Blackburn EH, Greider CW, Szostak JW (2006) Telomeres and telomerase: the path from maize, Tetrahymena and yeast to human cancer and aging. Nat Med 12:1133–1138.

Blank M, Tang Y, Yamashita M, Burkett SS, Cheng SY, Zhang YE (2012) A tumor suppressor function of Smurf2 associated with controlling chromatin landscape and genome stability through RNF20 Available at:. Nat Med 18:227–234.

Borroni AP, Emanuelli A, Shah PA, Ilić N, Apel-Sarid L, Paolini B, Manikoth Ayyathan D, Koganti P, Levy-Cohen G, Blank M (2018) Smurf2 regulates stability and the autophagic–lysosomal turnover of lamin A and its disease-associated form progerin. Aging Cell 17:1–12.

Brooks CL, Gu W (2003) Ubiquitination, phosphorylation and acetylation: The molecular basis for p53 regulation. Curr Opin Cell Biol 15:164–171.

Calhoun ME, Kurth D, Phinney AL, Long JM, Mouton PR, Ingram DK, Jucker M (1998) Hippocampal neuron and synaptic bouton number in aging C57BL/6 mice. Neurobiol Aging 19:599–606.

Carneiro MC, de Castro IP, Ferreira MG (2016) Telomeres in aging and disease: lessons from zebrafish. Dis Model Mech 9:737–748.

Cha B, Park Y, Hwang BN, Kim S, Jho E (2015) Protein arginine methyltransferase 1 methylates Smurf2 Available at:. Mol Cells 38:723–728.

Chandhoke AS, Karve K, Dadakhujaev S, Netherton S, Deng L, Bonni S (2016) The ubiquitin ligase Smurf2 suppresses TGFβ-induced epithelial–mesenchymal transition in a sumoylation-regulated manner. Cell Death Differ 23(5):876–888. https://doi.org/10.1038/cdd.2015.152.

Chen C, Matesic LE (2007) The Nedd4-like family of E3 ubiquitin ligases and cancer Available at:. Cancer Metastasis Rev 26:587–604.

Cong Y-S, Wright WE, Shay JW (2002) Human telomerase and its regulation. Microbiol Mol Biol Rev.

Das S, Chang C (2012) Regulation of early xenopus embryogenesis by smad ubiquitination regulatory factor 2 Available at:. Dev Dyn 241:1260–1273.

David D, Nair SA, Pillai MR (2013) Smurf E3 ubiquitin ligases at the cross roads of oncogenesis and tumor suppression. Biochimi. Biophys. Acta 1835(1):119–128. https://doi.org/10.1016/j.bbcan.2012.11.003.

de Oliveira GMT, Kist LW, Pereira TCB, Bortolotto JW, Paquete FL, de Oliveira EMN, Leite CE, Bonan CD, de Souza Basso NR, Papaleo RM, Bogo MR (2014) Transient modulation of acetylcholinesterase activity caused by exposure to dextran-coated iron oxide nanoparticles in brain of adult zebrafish. Comp Biochem Physiol Part C Toxicol Pharmacol 162:77–84. https://doi.org/10.1016/j.cbpc.2014.03.010.

Demaria M, Ohtani N, Youssef SA, Rodier F, Toussaint W, Mitchell JR, Laberge R-M, Vijg J, Van Steeg H, Dollé MET, Hoeijmakers JHJ, de Bruin A, Hara E, Campisi J (2014) An essential role for senescent cells in optimal wound healing through secretion of PDGF-AA Available at:. Dev Cell 31:722–733. Available from: https://linkinghub.elsevier.com/retrieve/pii/S1534580714007291.

Edelmann K, Glashauser L, Sprungala S, Hesl B, Fritschle M, Ninkovic J, Godinho L, Chapouton P (2013) Increased radial glia quiescence, decreased reactivation upon injury and unaltered neuroblast behavior underlie decreased neurogenesis in the aging zebrafish telencephalon Available at:. J Comp Neurol 521:3099–3115. Available from: http://doi.wiley.com/10.1002/cne.23347.

Emanuelli A, Manikoth Ayyathan D, Koganti P, Shah PA, Apel-Sarid L, Paolini B, Detroja R, Frenkel-Morgenstern M, Blank M (2019) Altered expression and localization of tumor suppressive E3 ubiquitin ligase SMURF2 in human prostate and breast cancer Available at:. Cancers (Basel) 11:556. Available from: https://www.mdpi.com/2072-6694/11/4/556.

Fulop T, Larbi A, Dupuis G, Le Page A, Frost EH, Cohen AA, Witkowski JM, Franceschi C (et) Immunosenescence and inflamm-aging as two sides of the same coin: friends or foes? Available at: Front Immunol 8.

Ganeshina O, Berry RW, Petralia RS, Nicholson DA, Geinisman Y (2004) Differences in the expression of AMPA and NMDA receptors between axospinous perforated and nonperforated synapses are related to the configuration and size of postsynaptic densities Available at:. J Comp Neurol 468:86–95. Available from: http://doi.wiley.com/10.1002/cne.10950.

Ganz J, Kroehne V, Freudenreich D, Machate A, Geffarth M, Braasch I, Kaslin J, Brand M (2014) Subdivisions of the adult zebrafish pallium based on molecular marker analysis. F1000Res 3:308.

Gao J, Wang W-Y, Mao Y-W, Gräff J, Guan J-S, Pan L, Mak G, Kim D, Su SC, Tsai L-H (2010) A novel pathway regulates memory and plasticity via SIRT1 and miR-134 Available at:. Nature 466:1105–1109. Available from: http://www.nature.com/articles/nature09271.

Glasauer SMK, Neuhauss SCF (2014) Whole-genome duplication in teleost fishes and its evolutionary consequences. Mol Genet Genomics 289:1045–1060.

Grandel H, Kaslin J, Ganz J, Wenzel I, Brand M (2006) Neural stem cells and neurogenesis in the adult zebrafish brain: Origin, proliferation dynamics, migration and cell fate Available at:. Dev Biol 295:263–277. Available from: https://linkinghub.elsevier.com/retrieve/pii/S0012160606002478.

Grönroos E, Hellman U, Heldin CH, Ericsson J (2002) Control of Smad7 stability by competition between acetylation and ubiquitination. Mol Cell 10:483–493.

Grönroos E, Terentiev AA, Punga T, Ericsson J (2004) YY1 inhibits the activation of the p53 tumor suppressor in response to genotoxic stress. Proc Natl Acad Sci 101:12165–12170.

Gu C, Xing Y, Jiang L, Chen M, Xu M, Yin Y, Li C, Yang Z, Yu L, Ma H (2013) Impaired cardiac SIRT1 activity by carbonyl stress contributes to aging-related ischemic intolerance Peng T, ed Available at:. PLoS One 8. Available from: https://dx.plos.org/10.1371/journal.pone.0074050 e74050.

Guarente L (2007) Sirtuins in aging and disease Available at:. Cold Spring Harb Symp Quant Biol 72:483–488. Available from: https://linkinghub.elsevier.com/retrieve/pii/S0092867406008920.

Hasegawa K, Yoshikawa K (2008) Necdin regulates p53 acetylation via Sirtuin1 to modulate DNA damage response in cortical neurons. J Neurosci 28:8772–8784.

Hata A, Chen Y-G (2016) TGF-β signaling from receptors to smads Available at:. Cold Spring Harb Perspect Biol 8. Available from: http://cshperspectives.cshlp.org/lookup/doi/10.1101/cshperspect.a022061 a022061.

Herskovits AZ, Guarente L (2014) SIRT1 in neurodevelopment and brain senescence. Neuron 81:471–483. https://doi.org/10.1016/j.neuron.2014.01.028.

Hoeijmakers JHJ (2009) DNA damage, aging, and cancer Available at:. N Engl J Med 361:1475–1485. Available from: http://www.nejm.org/doi/abs/10.1056/NEJMra0804615.

Hornsby PJ (2006) Short telomeres: cause or consequence of aging? Available at: Aging Cell 5:577–578. Available from: http://doi.wiley.com/10.1111/j.1474-9726.2006.00249.x.

Howe K et al (2013) The zebrafish reference genome sequence and its relationship to the human genome Available at:. Nature 496:498–503. Available from: http://www.nature.com/articles/nature12111.

Inoue K, Fry EA, Frazier DP (2016) Transcription factors that interact with p53 and Mdm2. Int J Cancer 138:1577–1585.

Ito A, Lai CH, Zhao X, Saito S, Hamilton MH, Appella E, Yao TP (2001) p300/CBP-mediated p53 acetylation is commonly induced by p53-activating agents and inhibited by MDM2. EMBO J 20:1331–1340.

Jeong HM, Lee SH, Yum J, Yeo C-Y, Lee KY (2014) Smurf2 regulates the degradation of YY1. Biochim Biophys Acta 1843 (9):2005–2011. https://doi.org/10.1016/j.bbamcr.2014.04.023.

Johnson SL, Weston JA (1995) Temperature-sensitive mutations that cause stage-specific defects in zebrafish fin regeneration. Genetics 141:1583–1595.

Karoglu ET, Halim DO, Erkaya B, Altaytas F, Arslan-Ergul A, Konu O, Adams MM (2017) Aging alters the molecular dynamics of synapses in a sexually dimorphic pattern in zebrafish (Danio rerio). Neurobiol Aging 54:10–21. https://doi.org/10.1016/j.neurobiolaging.2017.02.007.

Kavsak P, Rasmussen RK, Causing CG, Bonni S, Zhu H, Thomsen GH, Wrana JL (2000) Smad7 binds to Smurf2 to form an E3 ubiquitin ligase that targets the TGFβ receptor for degradation Available at:. Mol Cell 6:1365–1375. Available from: https://linkinghub.elsevier.com/retrieve/pii/S1097276500001349.

Kim D, Nguyen MD, Dobbin MM, Fischer A, Sananbenesi F, Rodgers JT, Delalle I, Baur JA, Sui G, Armour SM, Puigserver P, Sinclair DA, Tsai L-H (2007) SIRT1 deacetylase protects against neurodegeneration in models for Alzheimer's disease and amyotrophic lateral sclerosis Available at:. EMBO J 26:3169–3179. Available from: http://emboj.embopress.org/cgi/doi/10.1038/sj.emboj.7601758.

Kishi S, Uchiyama J, Baughman AM, Goto T, Lin MC, Tsai SB (2003) The zebrafish as a vertebrate model of functional aging and very gradual senescence. Exp Gerontol 38:777–786.

Kishi S, Bayliss PE, Uchiyama J, Koshimizu E, Qi J, Nanjappa P, Imamura S, Islam A, Neuberg D, Amsterdam A, Roberts TM (2008) The identification of zebrafish mutants showing alterations in senescence-associated biomarkers Mullins M, ed Available at:. PLoS Genet 4. Available from: http://dx.plos.org/10.1371/journal.pgen.1000152 e1000152.

Kitada M, Ogura Y, Koya D (2016) The protective role of Sirt1 in vascular tissue: its relationship to vascular aging and atherosclerosis. Aging (Albany NY) 8:2290–2307.

Kizil C, Kaslin J, Kroehne V, Brand M (2012) Adult neurogenesis and brain regeneration in zebrafish Available at:. Dev Neurobiol 72:429–461. Available from: http://doi.wiley.com/10.1002/dneu.20918.

Kong Y, Cui H, Zhang H (2011) Smurf2-mediated ubiquitination and degradation of Id1 regulates p16 expression during senescence Available at:. Aging Cell 10:1038–1046. Available from: http://doi.wiley.com/10.1111/j.1474-9726.2011.00746.x.

Krampert M, Chirasani SR, Wachs F-P, Aigner R, Bogdahn U, Yingling JM, Heldin C-H, Aigner L, Heuchel R (2010) Smad7 regulates the adult neural stem/progenitor cell pool in a transforming growth factor β- and bone morphogenetic protein-independent manner Available at:. Mol Cell Biol 30:3685–3694. Available from: http://mcb.asm.org/cgi/doi/10.1128/MCB.00434-09.

Krishnamurthy J, Torrice C, Ramsey MR, Kovalev GI, Al-Regaiey K, Su L, Sharpless NE (2004) Ink4a/Arf expression is a biomarker of aging Available at:. J Clin Invest 114:1299–1307. Available from: http://www.jci.org/articles/view/22475.

Krizhanovsky V, Xue W, Zender L, Yon M, Hernando E, Lowe SW (2008) Implications of cellular senescence in tissue damage response, tumor suppression, and stem cell biology Available at:. Cold Spring Harb Symp Quant Biol 73:513–522. Available from: http://symposium.cshlp.org/cgi/doi/10.1101/sqb.2008.73.048.

Kume S, Haneda M, Kanasaki K, Sugimoto T, Araki SI, Isshiki K, Isono M, Uzu T, Guarente L, Kashiwagi A, Koya D (2007) SIRT1 inhibits transforming growth factor β-induced apoptosis in glomerular mesangial cells via Smad7 deacetylation. J Biol Chem 282:151–158.

Lafontaine-Lacasse M, Richard D, Picard F (2010) Effects of age and gender on Sirt 1 mRNA expressions in the hypothalamus of the mouse. Neurosci Lett 480(1):1–3. https://doi.org/10.1016/j.neulet.2010.01.008.

Lee KY, Jewett KA, Chung HJ, Tsai N-P (2018) Loss of fragile X protein FMRP impairs homeostatic synaptic downscaling through tumor suppressor p53 and ubiquitin E3 ligase Nedd4-2 Available at:. Hum Mol Genet 27:2805–2816. Available from: https://academic.oup.com/hmg/article/27/16/2805/4996743.

Lessel D et al (2017) Dysfunction of the MDM2/p53 axis is linked to premature aging Available at:. J Clin Invest:3598–3608. Available from: https://www.jci.org/articles/view/92171.

Levy MZ, Allsopp RC, Futcher AB, Greider CW, Harley CB (1992) Telomere end-replication problem and cell aging. J Mol Biol 225:951–960.

Li MD, Burns TC, Morgan AA, Khatri P (2014) Integrated multi-cohort transcriptional meta-analysis of neurodegenerative diseases. Acta Neuropathol Commun 2:93.

Li M, Luo J, Brooks CL, Gu W (2002a) Acetylation of p53 inhibits its ubiquitination by Mdm2. J Biol Chem 277:50607–50611.

Li Y, Stockton ME, Eisinger BE, Zhao Y, Miller JL, Bhuiyan I, Gao Y, Wu Z, Peng J, Zhao X (2018) Reducing histone acetylation rescues cognitive deficits in a mouse model of Fragile X syndrome. Nat Commun 9(1). https://doi.org/10.1038/s41467-018-04869-3.

Li Q, Xiao H, Isobe K (2002b) Histone acetyltransferase activities of cAMP-regulated enhancer-binding protein and p300 in tissues of fetal, young, and old mice. J Gerontol Biol Sci 57A:B93–B98.

Liu R, Lei JX, Luo C, Lan X, Chi L, Deng P, Lei S, Ghribi O, Liu QY (2012) Increased EID1 nuclear translocation impairs synaptic plasticity and memory function associated with pathogenesis of Alzheimer's disease. Neurobiol Dis 45(3):902–912. https://doi.org/10.1016/j.nbd.2011.12.007.

López-Otín C, Blasco MA, Partridge L, Serrano M, Kroemer G (2013) The hallmarks of aging Available at:. Cell 153:1194–1217. Available from: https://linkinghub.elsevier.com/retrieve/pii/S0092867413006454.

Lord CJ, Ashworth A (2012) The DNA damage response and cancer therapy Available at:. Nature 481:287–294. Available from: http://www.nature.com/articles/nature10760.

Marschallinger J, Krampert M, Couillard-Despres S, Heuchel R, Bogdahn U, Aigner L (2014) Age-dependent and differential effects of Smad7ΔEx1 on neural progenitor cell proliferation and on neurogenesis. Exp Gerontol 57:149–154. https://doi.org/10.1016/j.exger.2014.05.011.

McHugh D, Gil J (2018) Senescence and aging: causes, consequences, and therapeutic avenues Available at:. J Cell Biol 217:65–77. Available from: http://www.jcb.org/lookup/doi/10.1083/jcb.201708092.

Michan S, Li Y, Chou MM-H, Parrella E, Ge H, Long JM, Allard JS, Lewis K, Miller M, Xu W, Mervis RF, Chen J, Guerin KI, Smith LEH, McBurney MW, Sinclair DA, Baudry M, de Cabo R, Longo VD (2010) SIRT1 is essential for normal cognitive function and synaptic plasticity Available at:. J Neurosci 30:9695–9707. Available from: http://www.jneurosci.org/cgi/doi/10.1523/JNEUROSCI.0027-10.2010.

Min S-W, Cho S-H, Zhou Y, Schroeder S, Haroutunian V, Seeley WW, Huang EJ, Shen Y, Masliah E, Mukherjee C, Meyers D, Cole PA, Ott M, Gan L (2010) Acetylation of Tau inhibits its degradation and contributes to tauopathy. Neuron 67:953–966. https://doi.org/10.1016/j.neuron.2010.08.044.

Muñoz-Espín D, Serrano M (2014) Cellular senescence: from physiology to pathology Available at:. Nat Rev Mol Cell Biol 15:482–496. Available from: http://www.nature.com/articles/nrm3823.

Nam R-H, Kim W, Lee C-J (2004) NMDA receptor-dependent long-term potentiation in the telencephalon of the zebrafish Available at:. Neurosci Lett 370:248–251. Available from: https://linkinghub.elsevier.com/retrieve/pii/S0304394004010481.

Newton IG, Forbes ME, Linville MC, Pang H, Tucker EW, Riddle DR, Brunso-Bechtold JK (2008) Effects of aging and caloric restriction on dentate gyrus synapses and glutamate receptor subunits. Neurobiol Aging 29(9):1308–1318. https://doi.org/10.1016/j.neurobiolaging.2007.03.009.

Ng M-C, Tang T-H, Ko M-C, Wu Y-J, Hsu C-P, Yang Y-L, Lu K-T (2012) Stimulation of the lateral division of the dorsal telencephalon induces synaptic plasticity in the medial division of adult zebrafish. Neurosci Lett 512(2):109–113. https://doi.org/10.1016/j.neulet.2012.01.070.

Nguyen P, Valanejad L, Cast A, Wright M, Garcia JM, El-Serag HB, Karns R, Timchenko NA (2018) Elimination of age-associated hepatic steatosis and correction of aging phenotype by inhibition of cdk4-C/EBPα-p300 axis. Cell Rep 24(6):1597–1609. https://doi.org/10.1016/j.celrep.2018.07.014.

Nie J, Xie P, Liu L, Xing G, Chang Z, Yin Y, Tian C, He F, Zhang L (2010) Smad ubiquitylation regulatory factor 1/2 (Smurf1/2) promotes p53 degradation by stabilizing the E3 ligase MDM2 Available at:. J Biol Chem 285:22818–22830. Available from: http://www.jbc.org/lookup/doi/10.1074/jbc.M110.126920.

Nüsslein-Volhard C, Dahm R (2002) Zebrafish: a practical approach, 1st ed. Oxford University Press. Available at: http://search.ebscohost.com/login.aspx?direct=true&db=cat00040a&AN=bilk.353363&site=eds-live.

Oliveira RF (2013) Mind the fish: zebrafish as a model in cognitive social neuroscience Available at:. Front Neural Circuits 7.

Ou H-L, Schumacher B (2018) DNA damage responses and p53 in the aging process Available at:. Blood 131:488–495. Available from: http://www.bloodjournal.org/lookup/doi/10.1182/blood-2017-07-746396.

Poe BH, Linville C, Riddle DR, Sonntag WE, Brunso-Bechtold JK (2001) Effects of age and insulin-like growth factor-1 on neuron and synapse numbers in area CA3 of hippocampus Available at:. Neuroscience 107:231–238. Available from: https://linkinghub.elsevier.com/retrieve/pii/S0306452201003414.

Poss KD (2002) Heart regeneration in zebrafish. Science (80-) 298:2188–2190 Available at: http://www.sciencemag.org/cgi/doi/10.1126/science.1077857.

Quintas A, de Solís AJ, Díez-Guerra FJ, Carrascosa JM, Bogónez E (2012) Age-associated decrease of SIRT1 expression in rat hippocampus. Exp Gerontol 47(2):198–201. https://doi.org/10.1016/j.exger.2011.11.010.

Ramkumar C, Kong Y, Cui H, Hao S, Jones SN, Gerstein RM, Zhang H (2012) Smurf2 regulates the senescence response and suppresses tumorigenesis in mice Available at:. Cancer Res 72:2714–2719. Available from: http://cancerres.aacrjournals.org/cgi/doi/10.1158/0008-5472.CAN-11-3773.

Ramkumar C, Kong Y, Trabucco SE, Gerstein RM, Zhang H (2014) Smurf2 regulates hematopoietic stem cell self-renewal and aging. Aging Cell 13:478–486.

Rapp PR, Gallagher M (1996) Preserved neuron number in the hippocampus of aged rats with spatial learning deficits Available at:. Proc Natl Acad Sci 93:9926–9930. Available from: http://www.pnas.org/cgi/doi/10.1073/pnas.93.18.9926.

Rapp PR, Deroche PS, Mao Y, Burwell RD (2002) Neuron number in the parahippocampal region is preserved in aged rats with spatial learning deficits Available at:. Cereb Cortex 12:1171–1179. Available from: https://academic.oup.com/cercor/article-lookup/doi/10.1093/cercor/12.11.1171.

Raz N (2002) Cognitive aging. In: Encyclopedia of the human brain. Elsevier. p. 829–838. https://doi.org/10.1016/B0-12-227210-2/00099-6.

Sasaki T (2015) Age-associated weight gain, leptin, and SIRT1: a possible role for hypothalamic SIRT1 in the prevention of weight gain and aging through modulation of leptin sensitivity Available at:. Front Endocrinol (Lausanne) 6:1–10. Available from: http://journal.frontiersin.org/Article/10.3389/fendo.2015.00109/abstract.

Saverino C, Gerlai R (2008) The social zebrafish: Behavioral responses to conspecific, heterospecific, and computer animated fish Available at:. Behav Brain Res 191:77–87. Available from: https://linkinghub.elsevier.com/retrieve/pii/S0166432808001460.

Sen P, Lan Y, Li CY, Sidoli S, Donahue G, Dou Z, Frederick B, Chen Q, Luense LJ, Garcia BA, Dang W, Johnson FB, Adams PD, Schultz DC, Berger SL (2019) Histone acetyltransferase p300 induces de novo super-enhancers to drive cellular senescence. Mol Cell 73(4):684–698.e8. https://doi.org/10.1016/j.molcel.2019.01.021.

Sezgin E, Azbazdar Y, Ng XW, Teh C, Simons K, Weidinger G, Wohland T, Eggeling C, Ozhan G (2017) Binding of canonical Wnt ligands to their receptor complexes occurs in ordered plasma membrane environments Available at:. FEBS J 284:2513–2526. Available from: http://doi.wiley.com/10.1111/febs.14139.

. Current Opinion in Immunology 22(4):507–513. https://doi.org/10.1016/j.coi.2010.05.003.

Shi L, Adams MM, Linville MC, Newton IG, Forbes ME, Long AB, Riddle DR, Brunso-Bechtold JK (2007) Caloric restriction eliminates the aging-related decline in NMDA and AMPA receptor subunits in the rat hippocampus and induces homeostasis Available at:. Exp Neurol 206:70–79. Available from: https://linkinghub.elsevier.com/retrieve/pii/S0014488607001380.

Shiu W-L, Huang K-R, Hung J-C, Wu J-L, Hong J-R (2016) Knockdown of zebrafish YY1a can downregulate the phosphatidylserine (PS) receptor expression, leading to induce the abnormal brain and heart development. J Biomed Sci 23(1). https://doi.org/10.1186/s12929-016-0248-1.

Simonsson M, Heldin CH, Ericsson J, Grönroos E (2005) The balance between acetylation and deacetylation controls Smad7 stability. J Biol Chem 280:21797–21803.

Solomon JM, Pasupuleti R, Xu L, McDonagh T, Curtis R, DiStefano PS, Huber LJ (2006) Inhibition of SIRT1 catalytic activity increases p53 acetylation but does not alter cell survival following DNA damage Available at:. Mol Cell Biol 26:28–38. Available from: http://mcb.asm.org/cgi/doi/10.1128/MCB.26.1.28-38.2006.

Sui G, Affar El Bachir, Shi Y, Brignone C, Wall NR, Yin P, Donohoe M, Luke MP, Calvo D, Grossman SR, Shi Y (2004) Yin Yang 1 is a negative regulator of p53 Available at:. Cell 117:859–872. Available from: https://linkinghub.elsevier.com/retrieve/pii/S0092867404005446.

Szklarczyk D, Gable AL, Lyon D, Junge A, Wyder S, Huerta-Cepas J, Simonovic M, Doncheva NT, Morris JH, Bork P, Jensen LJ, von Mering C (2019) STRING v11: protein–protein association networks with increased coverage, supporting functional discovery in genome-wide experimental datasets Available at:. Nucleic Acids Res 47:D607–D613. Available from: https://academic.oup.com/nar/article/47/D1/D607/5198476.

Tedeschi A, Di Giovanni S (2009) The non-apoptotic role of p53 in neuronal biology: enlightening the dark side of the moon Available at:. EMBO Rep 10:576–583. Available from: http://embor.embopress.org/cgi/doi/10.1038/embor.2009.89.

Tominaga K, Suzuki HI (2019) TGF-β signaling in cellular senescence and aging-related pathology Available at:. Int J Mol Sci 20:5002. Available from: https://www.mdpi.com/1422-0067/20/20/5002.

Ullmann JFP, Cowin G, Kurniawan ND, Collin SP (2010) A three-dimensional digital atlas of the zebrafish brain. NeuroImage 51(1):76–82. https://doi.org/10.1016/j.neuroimage.2010.01.086.

Van Houcke J, De Groef L, Dekeyster E, Moons L (2015) The zebrafish as a gerontology model in nervous system aging, disease, and repair. Ageing Res Rev 24:358–368. https://doi.org/10.1016/j.arr.2015.10.004.

VanGuilder HD, Yan H, Farley JA, Sonntag WE, Freeman WM (2010) Aging alters the expression of neurotransmission-regulating proteins in the hippocampal synaptoproteome Available at:. J Neurochem 113:1577–1588. Available from: http://doi.wiley.com/10.1111/j.1471-4159.2010.06719.x.

VanGuilder HD, Farley JA, Yan H, Van Kirk CA, Mitschelen M, Sonntag WE, Freeman WM (2011) Hippocampal dysregulation of synaptic plasticity-associated proteins with age-related cognitive decline. Neurobiol Dis 43(1):201–212. https://doi.org/10.1016/j.nbd.2011.03.012.

Varga ZM, Matthews M (2012) Anesthesia and Euthanasia in Zebrafish. ILAR J 53(2):192–204. https://doi.org/10.1093/ilar.53.2.192.

Vaziri H, Dessain SK, Eaton EN, Imai S-I, Frye RA, Pandita TK, Guarente L, Weinberg RA (2001) hSIR2SIRT1 functions as an NAD-dependent p53 deacetylase Available at:. Cell 107:149–159. Available from: http://www.nature.com/articles/nsmb.1604.

Wiesner S, Ogunjimi AA, Wang H-R, Rotin D, Sicheri F, Wrana JL, Forman-Kay JD (2007) Autoinhibition of the HECT-type ubiquitin ligase Smurf2 through Its C2 domain Available at:. Cell 130:651–662. Available from: https://linkinghub.elsevier.com/retrieve/pii/S0092867407009002.

Wright WE, Piatyszek MA, Rainey WE, Byrd W, Shay JW (1996) Telomerase activity in human germline and embryonic tissues and cells Available at:. Dev Genet 18:173–179. Available from: http://doi.wiley.com/10.1002/%28SICI%291520-6408%281996%2918%3A2%3C173%3A%3AAID-DVG10%3E3.0.CO%3B2-3.

Wu YJ, Chen YL, Tang TH, Ng MC, Amstislavskaya TG, Tikhonova MA, Yang YL, Lu KT (2017) Unilateral stimulation of the lateral division of the dorsal telencephalon induces synaptic plasticity in the bilateral medial division of zebrafish. Sci Rep 7. https://doi.org/10.1038/s41598-017-08093-9.

Wu D, Prives C (2018) Relevance of the p53–MDM2 axis to aging. Cell Death Differ 25:169–179. https://doi.org/10.1038/cdd.2017.187.

Wullimann MF, Rupp B, Reichert H (1996) Neuroanatomy of the zebrafish brain. Basel: Birkhäuser Basel. Available at: http://link.springer.com/10.1007/978-3-0348-8979-7.

Yan X, Liu Z, Chen Y (2009) Regulation of TGF-β signaling by Smad7 Available at:. Acta Biochim Biophys Sin (Shanghai) 41:263–272. Available from: https://academic.oup.com/abbs/article-lookup/doi/10.1093/abbs/gmp018.

Yao Y-L, Yang W-M, Seto E (2001) Regulation of transcription factor YY1 by acetylation and deacetylation Available at:. Mol Cell Biol 21:5979–5991. Available from: http://mcb.asm.org/cgi/doi/10.1128/MCB.21.17.5979-5991.2001.

Yi J, Luo J (2010) SIRT1 and p53, effect on cancer, senescence and beyond Available at:. Biochim Biophys Acta 1804:1684–1689. https://doi.org/10.1016/j.bbapap.2010.05.002.

Yu L, Tucci V, Kishi S, Zhdanova IV (2006) Cognitive aging in zebrafish Miall C, ed Available at:. PLoS One 1. Available from: https://dx.plos.org/10.1371/journal.pone.0000014 e14.

Yuan Y, Cruzat VF, Newshome P, Cheng J, Chen Y, Lu Y (2016) Regulation of SIRT1 in aging: Roles in mitochondrial function and biogenesis Available at:. Mech Ageing Dev 155:10–21. https://doi.org/10.1016/j.mad.2016.02.003.

Zhang Y, Chang C, Gehling DJ, Hemmati-Brivanlou A, Derynck R (2001) Regulation of Smad degradation and activity by Smurf2, an E3 ubiquitin ligase Available at:. Proc Natl Acad Sci 98:974–979. Available from: http://www.pnas.org/cgi/doi/10.1073/pnas.98.3.974.

Zhang H, Cohen SN (2004) Smurf2 up-regulation activates telomere-dependent senescence Available at:. Genes Dev 18:3028–3040. Available from: http://www.genesdev.org/cgi/doi/10.1101/gad.1253004.

(Received 25 November 2019, Accepted 1 April 2020)
(Available online 8 April 2020)